

**Investigation into Possible Mechanisms of Light
Pollution Flashover of 275kV Transmission Lines as
a Cause of Unknown Outages**

Kevin Kleinhans



**Thesis presented in fulfilment of the requirements for the degree of
Master of Engineering at the University of Stellenbosch**

**Supervisor:
Dr. J.P. Holtzhausen**

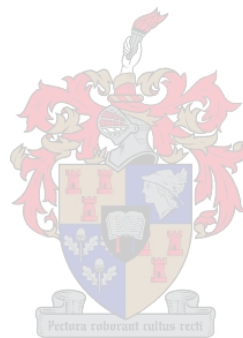
April 2005

Declaration

I, the undersigned, hereby declare that the work contained in this thesis is my own original work and that I have not previously in its entirety or in part submitted it at any university for a degree.

Signature:.....

Date:.....



Abstract

The cause of the largest number of faults on the Eskom main transmission system is unknown. It is believed that a non-uniform pollution layer along an insulator string is the reason for these anomalous flashovers. This non-uniform pollution layer results in the highest electric field strength, and thus the highest voltage, across the cleanest and driest discs. There thus exists a strong possibility that the anomalous flashover phenomenon is caused by a combination of mechanisms involving the pollution and air breakdown flashover mechanisms. This research project attempted to prove that flashover of the insulators is possible in accordance with the above model. Various experiments were set up in the high voltage laboratory and at a natural test site with a low source impedance supply attempting to simulate the conditions that lead to flashover in accordance with the hypothesis. All the tests done have not proven the non-uniform light pollution flashover mechanism successfully. However, future research has proposed an air breakdown flashover mechanism in light pollution conditions where the polluted part of the insulator string has a specific non-uniform distribution. Full scale testing in conditions similar to the normal operating conditions is proposed to prove the validity of this new hypothesis.



Opsomming

Die oorsaak van die grootste aantal foute op die Eskom transmissienetwerk is onbekend. Dit word beweer dat 'n nie-uniforme besoedelingslaag die oorsaak is van hierdie foute. Die nie-uniforme besoedelingslaag veroorsaak die hoogste elektriese veldsterkte en dus die hoogste potensiaal oor die skoonste en droogste skywe in die isolator string. Daar bestaan dus 'n groot moontlikheid dat die onbekende oorvonkings verskynsel veroorsaak word deur 'n kombinasie van meganismes wat die besoedeling en lug oorvonking meganismes bevat. Hierdie navorsingsprojek het beoog om te bewys dat die oorvonking van die isolators moontlik is op grond van die bogenoemde model. 'n Verskeidenheid eksperimente was in die hoogspannings laboratorium en by 'n natuurlike toetsfasiliteit opgestel om die kondisies wat tot oorvonking lei volgens die hipotese te probeer simuleer. Al die toetse wat gedoen is kon nie die nie-uniforme ligte besoedelings meganisme suksesvol bewys nie. Daaropvolgende navorsing het 'n lug-oorvonkingsmeganisme in ligte besoedelings kondisies waar die besoedelde deel van die isolator string 'n spesifieke nie-uniforme distribusie bevat, beweer. Volskaalse toetse word voorgestel om gedoen te word om die geldigheid van hierdie nuwe hipotese te bewys.



Acknowledgements

Special thanks must be given to:

God, my family and friends for your love, help and never ending support;

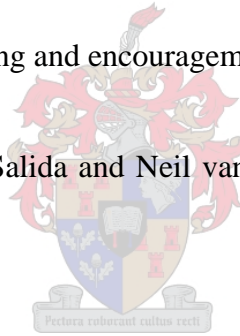
Dr. Koos Holtzhausen and Dr. Wallace Vosloo for your help and guidance throughout this research, believing in me to the end;

Miss Liezl van Wyk for your encouragement, especially during the final phase of the research;

Mr. Tony Britten for your ongoing support and interest in my research;

Carike for your love, caring and encouragement throughout;

Petrus Pieterse, Stanley Salida and Neil van der Merwe for your help during the research.



Do not cry if the Sun sets at the end of the day,
because the tears will not let you enjoy the beauty of the Stars.

Table of contents

	Page
1. Introduction	1
1.1 Project Motivation	1
1.2 Project Description	4
1.3 Thesis Structure	5
2. A Review of Insulator Flashover Processes	6
2.1 Air Breakdown	6
2.2 Pollution flashover mechanism	10
2.2.1 Formation of contamination layers	11
2.2.2 Insulator wetting	12
2.2.3 Dry band arcing	13
2.2.4 Insulator pollution severity	15
2.3 Bird streamer flashovers	16
2.4 Fire induced flashovers	17
2.5 Hypothesis: Air breakdown, assisted by non-uniform light pollution along the string	18
3. Laboratory Investigations	20
3.1 Introduction	20
3.2 The effect of pollution on the underside of the discs of a 4-disc I-string	20
3.2.1 Flashover tests	20
3.2.2 Measurements taken at 50kV: Potential and field strength distribution	24
3.2.2.1 Voltage distribution across the string	24
3.2.2.2 Electric field along the string	27
3.2.2.3 Electric field inside fog chamber	30
3.3 The effect of two clean discs in a lightly-polluted 16-disc I-string	31
3.3.1 Laboratory tests	31

3.3.1.1	Flashover tests	32
3.3.1.2	Voltage and electric field measurements	33
3.3.2	Night tests to investigate heating of discs adjacent to the current carrying conductor	38
3.3.2.1	The influence of conductor temperature on insulator performance	38
3.3.2.1.1	Temperature measurements	38
3.3.2.1.2	Resistance measurements across string	41
3.4	The effect of V-strings	42
3.4.1	Tests on the 25kV traction insulators	42
3.4.1.1	Pre-deposited pollution	43
3.4.1.2	Non-uniform pollution	43
3.4.1.3	Condensation using dry-ice chamber	44
3.4.2	Flashover tests on a 32-disc V-string	46
3.4.3	Tests done on 275kV tower	47
3.5	General summary of laboratory tests	47
4.	The effect of a spark gap in series with a polluted insulator string	49
4.1	Technical layout and setup of experiments at KIPTS	49
4.2	Results of measurements	51
4.3	Discussion	54
4.4	Conclusions	56
5.	Conclusions	58
6.	Bibliography	62
	Appendix A: Type of glass insulator used in tests	69
	Appendix B: 275kV tower	70
	Appendix C: Pollution test methods	72

List of Abbreviations

MTS	Main Transmission System
kV	kilo Volts
mm/kV	millimeters per kilo Volt
NETFA	SABS HV test facility
EPRI	Electric Power Research Institute
HV	High Voltage
ESDD	Equivalent Salt Deposit Density
AC	Alternating Current
DC	Direct Current
NaCl	Sodium Chloride
ESVM	Electrostatic Voltmeter
$T_s(K)$	Saturation Temperature
KIPTS	Koeberg Insulator Pollution Test Station
OLCA	On-line Leakage Current Analyser
VT	Voltage Transformer
L-L	line to line
L-G	line to ground
DAD	Dry Arcing Distance



Keywords

Alternating current

Creepage distance

Dry band

Equivalent Salt Deposition Density

Electrostatic voltmeter

Fog chamber

Flashover mechanism

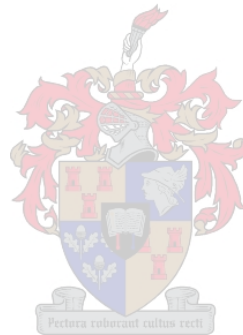
High voltage

HV laboratory

NaCl – Sodium chloride (common salt)

Non-uniform pollution layer

Wetting



List of Figures

<i>Number</i>	<i>Description</i>	<i>Page</i>
Figure 1.1:	Classification of faults between 1993 & 1998 [Britten 1999]	2
Figure 1.2:	Histogram of fault times for several major rogue lines (Note: Sample is 143 faults from 10 lines)	3
Figure 2.1:	Distribution of charge carriers in an avalanche	7
Figure 2.2:	Pre-breakdown Corona and sparkover w.r.t. time [Ryan]	8
Figure 2.3:	Schematic of events leading to contamination flashover [Guror]	11
Figure 2.4:	Schematic of dry band arcing on a polluted insulator [Guror]	14
Figure 3.1:	Schematic diagram showing the connection of the 350kV test transformer	21
Figure 3.2:	Glass insulator with copper wire wound around pin and connected to outer diameter	21
Figure 3.3:	Average % reduction in creepage distance, dry arc distance (DAD) and flashover voltage for number of discs partially shorted	23
Figure 3.4:	Schematic diagram of voltage measurement setup	24
Figure 3.5:	Glass insulator with pollution paste at the bottom of the disc	25
Figure 3.6:	Graphs of ESVM readings with some amount of the discs shorted underneath with aluminium foil	25
Figure 3.7:	Graphs of ESVM readings with some amount of discs shorted underneath with pollution paste	26
Figure 3.8:	Schematic diagram of electric field measurement setup	28
Figure 3.9:	Graphs of electric field readings with some amount of discs shorted underneath with aluminium foil	28
Figure 3.10:	Graphs of electric field readings with some amount of discs shorted underneath with pollution paste	29
Figure 3.11:	Schematic diagram of fog chamber setup	30
Figure 3.12:	Local flashover across two clean discs at the dead end	32

List of Figures

Figure 3.13:	Local flashover across two clean discs in the middle	32
Figure 3.14:	Local flashover across two clean discs at the live end	32
Figure 3.15:	Schematic diagram of voltage measurement along insulator string – 1	33
Figure 3.16:	Schematic diagram of voltage measurement along insulator string – 2	34
Figure 3.17:	Voltage distribution over the insulator string with the clean discs at the dead end (disc 1 is at the dead end)	35
Figure 3.18:	Electric field along the insulator string with the clean discs at the dead end (disc 1 is at the dead end)	35
Figure 3.19:	Voltage distribution over the insulator string with the clean discs in the middle (disc 1 is at the dead end)	35
Figure 3.20:	Electric field along the insulator string with the clean discs in the middle (disc 1 is at the dead end)	35
Figure 3.21:	Voltage distribution over the insulator string with the clean discs at the live end of the insulator string (disc 1 is at the dead end)	36
Figure 3.22:	Electric field along the insulator string with the clean discs at the live end of the insulator string (disc 1 is at the dead end)	36
Figure 3.23:	Equivalent diagram for 16-disc insulator string with the clean discs at the ground end	37
Figure 3.24:	Experimental setup of temperature and resistance readings	39
Figure 3.25:	Temperature readings with conductor at 75°C	40
Figure 3.26:	Temperature readings with conductor at 60°C	40
Figure 3.27:	Resistance measurements with conductor at 75°C	41
Figure 3.28:	Experimental setup of the 25kV traction insulators	43
Figure 3.29:	Experimental setup of the dry-ice chamber	44
Figure 3.30:	Arc initialisation	46
Figure 3.31:	Convection of arc	46
Figure 4.1:	Schematic diagram of test setup	49
Figure 4.2:	Actual setup at KIPTS	50
Figure 4.3:	Spark gap used in experiment	51

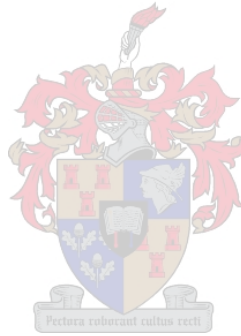
List of Figures

Figure 4.4:	Leakage current over string A – oscilloscope	52
Figure 4.5:	Leakage current over string A – Corocam and OLCA	52
Figure 4.6:	Small capacitive leakage current over string B – oscilloscope	53
Figure 4.7:	Spark gap flashover on string B – oscilloscope	53
Figure 4.8:	Equivalent diagram of the two insulator strings	54
Figure B.1	275kV tower window set up outside the High Voltage Laboratory	70
Figure B.2	Schematic of 275kV tower, from the waist up	71



List of Tables

<i>Number</i>	<i>Description</i>	<i>Page</i>
Table 1.1:	Line lengths of different operating voltages in the Eskom MTS	1
Table 2.1:	Comparison of magnitude of forces responsible for insulator contamination (particle size=5 μ m) [Guror]	12
Table 2.2:	Pollution levels and typical environments	16
Table 3.1:	Flashover voltages of 4-disc insulator string with different discs shorted underneath with copper	22
Table C.1:	Comparison of pollution test methods	74



Introduction

1.1 Project Motivation

Eskom, the national electricity supply utility in South Africa, operates a vast network of electricity transmission lines, forming its main transmission system (MTS). Details of the lines at the various voltage levels are given in Table 1.1.

Extensive fault statistics are kept up to date. An analysis of these statistics is given in Figure 1.1. Note that the largest number of faults on the MTS has occurred in the “unknown” category. Although some of the causes of faults in this group have since been identified, it can be stated that the reporting error here is about 10-15% of the total number of faults. This implies that the range of unknown faults is probably some 23 to 38% of the total number of faults. Lines contributing significantly to the overall number of faults arising from unknown causes have become known as “rogue” lines.

Operating voltage (kV)	Line lengths (km)
220	1 239
275	7 130
400	14 216
765	862

Table 1.1: Line lengths of different operating voltages in the Eskom MTS

In specific cases it has, for example, been found that inadequate clearances (jumper to tower, at angle or strain towers) and bird droppings were the predominant causes of flashover. These problems have been corrected quite easily. Despite this, it was considered, from incidents where birds were unlikely to have been a factor, that there could be an underlying mechanism which subjects glass cap and pin insulator strings to flashovers.

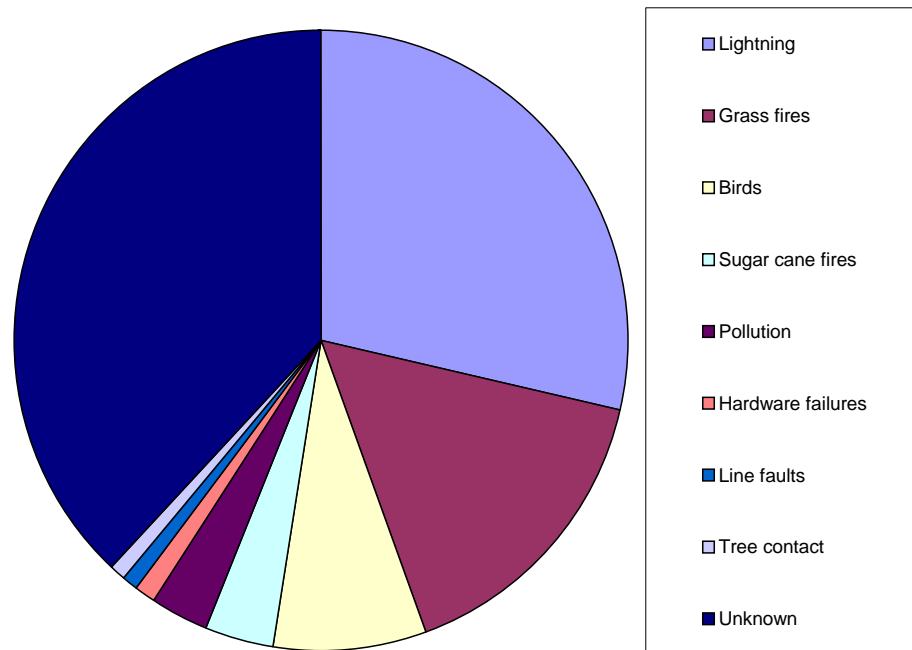


Figure 1.1: Classification of faults between 1993 & 1998 [Britten 1999]

Initial studies [Britten 1999] of faults in the unknown category problem revealed the following common factors:

- (a) The problem lines occur in many diverse geographical areas of South Africa from dry to moist climates, near sea level to high altitude.
- (b) Some 20% of all faults (i.e. about 50% of these anomalous faults) occur between about 22:00 and 06:00. The fact that as birds are not generally active during this period, it is concluded that another factor must be responsible for these flashovers. (See figure 1.2)
- (c) It is improbable that switching surges are the cause of the flashovers. This is simply reasoned as follows: the design rate of one outage in 10^4 switching surges would imply that, for 1000 flashovers, a total of some 10^7 switching (circuit breaker) operations already would have to occur in a 5 year period. The actual number of operations in this time is probably of the order of a few tens of thousands. Hence this factor has been discounted, as the number of faults are not comparable with the number of switching operations.

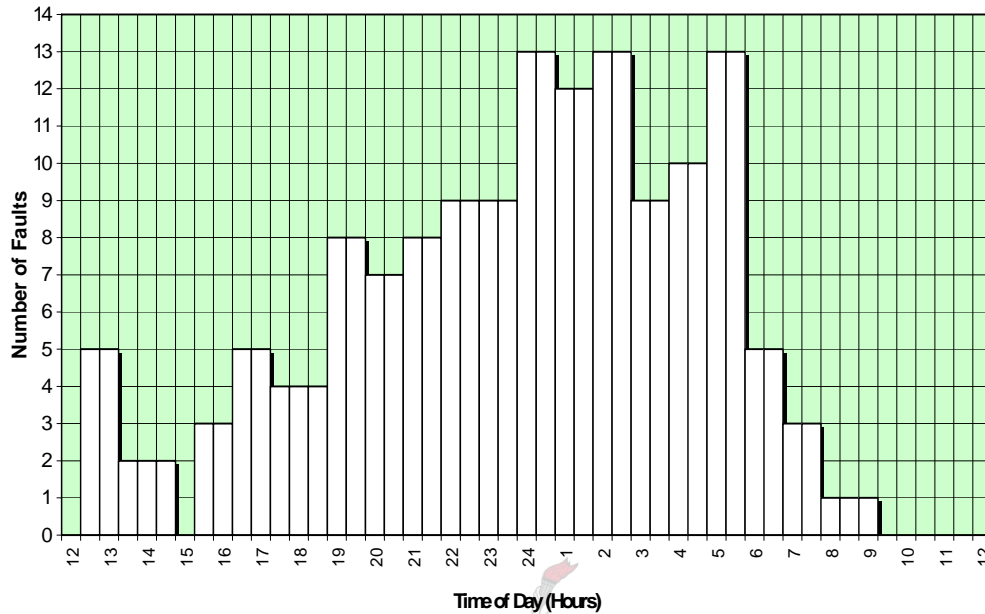


Figure 1.2: Histogram of fault times for several major rogue lines
 (Note: Sample is 143 faults from 10 lines.) [Britten 1997]

The factors, which so far appear to be common to these anomalous flashovers, are:

- a) These problems occurred mainly on lines using glass cap and pin insulators. (Although a few, about 2, anomalous flashovers are known to have occurred across polymeric strings, the mechanism is believed to be different from that of glass.)
- b) These faults occurred in regions classed as light pollution severity in terms of IEC-60815.
- c) In some cases the under-skirts of the insulators were polluted with the upper surfaces usually clean.
- d) The distribution of the pollution along the insulator string was often non-uniform, the highest being at the live end.

- e) These faults occurred predominantly on the centre phase V-string insulators and were mainly of a transient nature.
- f) The relative humidity appears to have been sustained at levels exceeding 75% for some hours prior to flashover [Britten 1997].
- g) The presence of corona streamers on the live-end insulators and hardware was reported to occur sometimes on a few of these lines.
- h) The insulators on the majority of the lines were dimensioned such that the specific creepage at U_{\max} was 14,9 mm/kV for the 275 kV lines and 15,3 mm/kV for the 400 kV lines. It should be noted that this creepage length is marginal, even in the case of light pollution [IEC-60815].

The high occurrence of flashovers in the period 22:00 – 06:00 has led to the speculative hypothesis that light pollution, moistened by a high, sustained, prevailing relative humidity, could be an underlying cause of these flashovers. This is partially supported by past research [Rizk 1970, EPRI 1982, Kawamura 1973 and Zedan 1983], and field observations particularly on 400 kV lines in the Eskom network. Birds are known to be the major cause of faults on certain lines, and are still considered together with the pollution phenomenon to be the most significant cause of these unexplained flashovers [Taylor].

One possible explanation for these flashovers involves the presence of a non-uniform light pollution layer on the surface [Guror 1997]. The presence of a non-uniform conducting layer on the insulator surface may distort the field distribution to such an extent that flashover may be initiated.

1.2 Project Description

The aim of this research project is to prove that flashover of the insulators are possible in accordance with the above model. For this analysis, 275kV line conditions will be considered, operating under the same conditions as on the lines in question.

Various experiments were set up in the high voltage laboratory attempting to simulate the conditions that lead to flashover in accordance with the hypothesis. The effect of the non-uniform pollution of each disc of the string was simulated and the field distribution and the flashover voltage were obtained. Further the effect of different pollution degrees of the discs along the string were also investigated. Several of these tests were done using V-strings.

It will also be necessary to prove that the flashover mechanism is not due to the normal pollution mechanism.

1.3 Thesis Structure

In chapter 2 the various pollution and air breakdown flashover mechanisms are compared. The hypothesised light pollution flashover mechanism is also discussed.

In chapter 3 all laboratory experiments done at the High Voltage Laboratory of the University of Stellenbosch are discussed. The effects of various conductive surfaces on the underside of the insulator discs are investigated by means of laboratory experiments on a 4-disc insulator string. These experiments are then extended to a 16-disc insulator string. The effect of two clean insulators in a lightly polluted string is investigated. The possibility of the discs adjacent to the current carrying conductor becoming dry is also investigated. Laboratory tests are then done to investigate the performance of V-strings under the above conditions.

In chapter 4, tests at an outside test site are described. In these tests the aspects dealt with in chapter 3 in the laboratory are investigated at a natural test site with a low source impedance supply.

All results and discussions are concluded upon in chapter 5. A way forward is also suggested.

A Review of Insulator Flashover Processes

In this chapter a literature survey is presented on the different models of insulator flashover.

It is important to have a good understanding of the pollution and air breakdown flashover phenomena in order to have a better grasp of the anomalous flashover problem.

2.1 Air breakdown

Electrical breakdown of air can occur in two ways: partial breakdown or corona over part of an airgap or complete breakdown causing a spark. Depending on the source supplying this spark, it can ultimately evolve into an arc. [Abdel-Salam]

The process of electrical breakdown is always initiated by the ionisation of air. When an electric field E is applied across an airgap, the electrons accelerate towards the positive anode. This happens because the electron acquires enough energy to ionise a gas molecule by collision. As a new electron is freed, the process repeats itself, causing this discharge to become self-sustaining. As this process is repeated, an electron avalanche is formed (see Figure 2.1). As successive avalanches are formed, a rapid current growth is experienced, leading to an air breakdown.

For the development of these avalanches into flashover, two mechanisms occur: the Townsend mechanism and the streamer mechanism.

The Townsend mechanism comprises the formation of several parallel avalanches, initiated by cathode phenomena or photo-ionisation.

Contrary to the Townsend mechanism, another mechanism was suggested [Loeb 1965] to show how a series of consecutive avalanches is generated, specifically in long gaps, where the sparks seem to branch and have an irregular growth. This streamer mechanism suggests that the discharge develop directly from a single

avalanche, which then transforms into a streamer. When the conductivity grows, the breakdown occurs through its channel. The photo-ionisation of the gas molecules in front of the streamer and the strengthening of the electric field by the charge are evident. This charge produces a distortion of the field in the airgap.

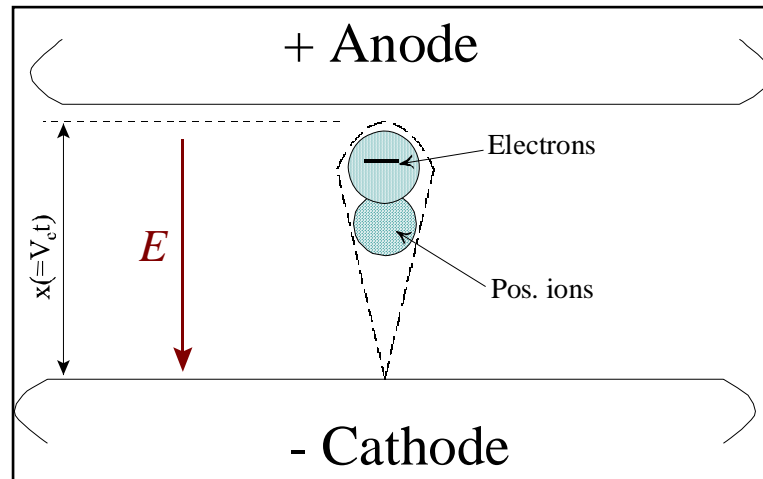


Figure 2.1: Distribution of charge carriers in an avalanche

Thus, in a uniform field, under specific conditions, both mechanisms are valid.

However, in non-uniform fields, the streamer mechanism is widely used to explain breakdown.

The non-uniform field needs much lower electric field strength to produce similar discharges than in a uniform field, as corona sets in and develops into flashover. In an AC field, the ions in the gas would be subjected to a slow alternating field relative to air breakdown. In the transmission system, corona precedes breakdown. The shape of the electrodes influences the maximum field, thus the corona onset voltage. In a non-uniform gap, corona appears at the electrodes with a small radius of curvature, where the fields are the highest. At increasing voltages, streamers develop that initiate flashover. Thus the breakdown voltage is mainly dependent on the gap length.

In larger non-uniform gaps, leaders are formed during the pre-breakdown phase. The development of such a leader is shown in Figure 2.2 for the case of a rising voltage such as a switching impulse or a 50Hz half cycle. More streamers are propagated from the tip of these advancing leaders (Figure 2.2). In this model, avalanches occur

at both electrodes, although the degree of ionisation is much more extensive at the anode (region B of Figure 2.2). This phenomenon is because negative corona is much less intensive than positive corona. Sparkover occurs when a conducting channel is established across the airgap, i.e. when the two ionisation regions meet.

The breakdown phenomena for a clean insulator string is similar to those appearing in an airgap. In any high voltage system, the dielectric strength of the insulator surface is usually the weakest part of the insulation [Ryan].

The connection length of a 275kV 16-disc glass insulator string is approximately 2 metres. The insulator string can be seen as having the characteristics of a rod gap. With this fact in mind, the AC spark over voltage gradient of this dimension is in the order of 0.5MV/m, thus needing 1000kV [Kind and Kärner]. The quoted dry flashover voltage for a 16-disc insulator string from the manufacturer [Pilkington Catalogue] is 780kV.

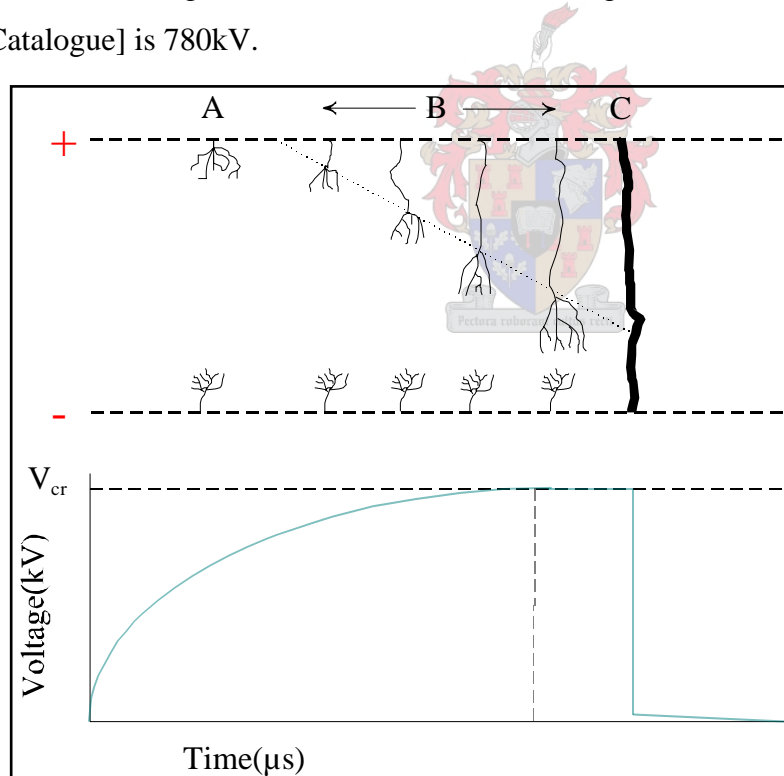


Figure 2.2: Pre-breakdown Corona and sparkover w.r.t. time [Ryan]

(A – initial streamer corona B – Leader growth phase C – Breakdown)

The phase to ground voltage on a 275kV transmission line is only 160kV. It can thus be said with certainty that under normal power frequency voltage conditions, air

breakdown of a clean insulator string is for all practical purposes impossible. Flashover of a clean insulator string would therefore only be possible due to switching surges, or lightning.

Voltage distribution along an insulator string is non-uniform. Corona and flashover will start at the disc closest to the live end.

Mention must be made of the calculated voltage across the insulator string and how it was derived.

Voltage distribution calculated along the insulator string

The closest calculated representation of an insulator string was found using the formula in Weeks (pp. 183 – 187). Using this representation, the voltage distribution along an insulator string with z glass insulators is:

$$V_n = \frac{V_0}{\beta^2 \sinh \beta z} \left(\frac{c}{C} \sinh \beta n + \frac{k}{C} \sinh \beta(n-z) + \frac{k}{C} \sinh \beta z \right)$$

where

V_n = the voltage across n units from ground

V_0 = the voltage across all the z units

$$\beta = \sqrt{\frac{c+k}{C}}$$

C = the capacitance between an individual cap and pin

c = the capacitance of one unit to ground

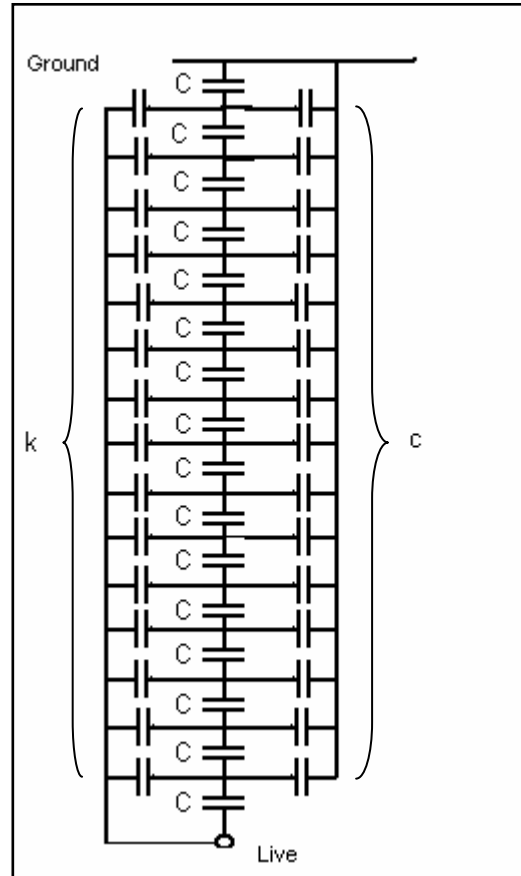
k = the capacitance of one unit to the high voltage conductor.

In the practical application of this calculation to these experiments, the stray capacitance to the live conductor, k, was considered to be negligible. Using this generalisation, the equation for the voltage across an individual unit is then simplified to:

$$V_n = V_0 \frac{\sinh \alpha n}{\sinh \alpha z}$$

where

$$\alpha = \sqrt{\frac{c}{C}}$$



The capacitance across one glass insulator was measured at 30 pF, and the stray capacitance of one unit to ground was averaged at 2.2pF [Weeks]. Since V_0 and z are also known values, the voltage across each individual insulator could be established.

2.2 Pollution flashover mechanism

High-voltage insulators are normally exposed to air and all of its impurities. If a contamination layer develops on the surface of such an insulator, its electric strength can be substantially reduced by as much as 80%. The events leading to contamination flashover of outdoor insulators are shown in Figure 2.3. A brief description of the pollution flashover process is given below.

2.2.1 Formation of contamination layers

According to Guror, the main forces acting on a dust particle near an energised insulator are gravity, wind and electric field. The force due to wind is the strongest. The electric field (E) causes a force consisting of two components: one proportional to E, and another proportional to E^2 due to the divergence of the electric field. In the case of AC lines, only the force due to field divergence always results in a force in the direction of increased field.

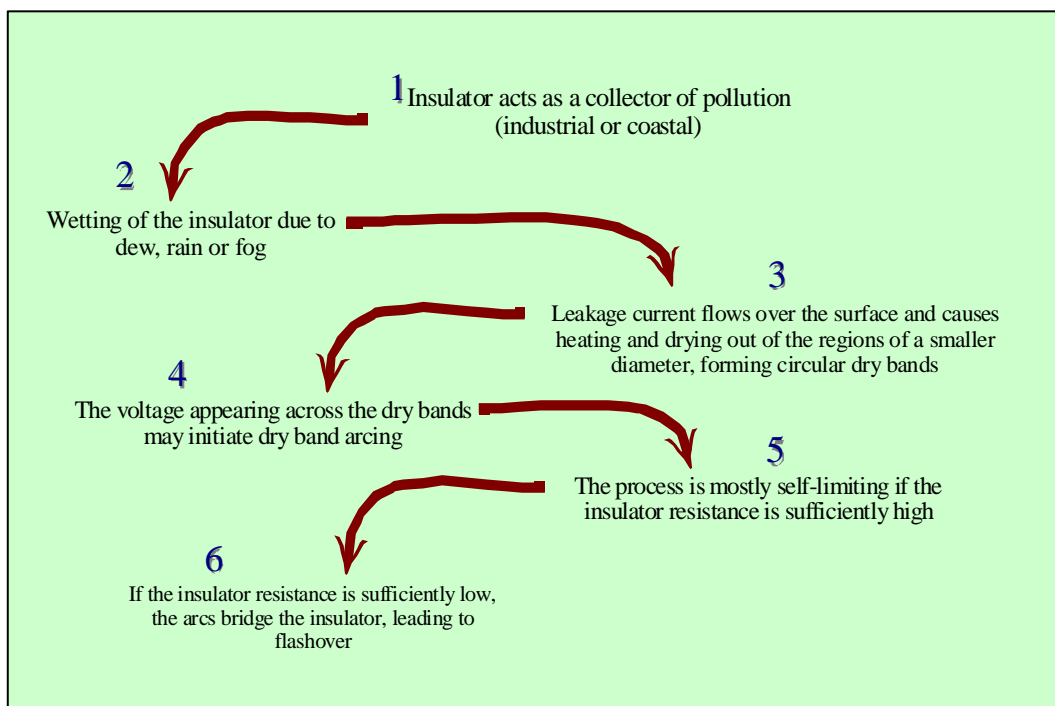


Figure 2.3: Schematic of events leading to contamination flashover [Guror]

Guror compared the magnitude of the forces on a dust particle, as shown in Table 2.1. The most important factor affecting contamination is wind. The aerodynamics of wind flow around an insulator string together with the fact that the highest field strength occurs near the live end discs result in the lower section of an insulator string being more polluted than the rest of the string. There are many types of contaminants in the field. The type and amount accumulated on the insulator depends on the service area.

Type of force	Relative Magnitude
Gravity	1 pu (reference)
Voltage stress ($E=2\text{kV/cm DC}$)	10
Field divergence ($E^2=0.2\text{kV}^2/\text{cm}^2$)	0.0001
Wind (2m/s)	1 000
Wind (5m/s)	2 000
Wind (10m/s)	3 000

Table 2.1: Comparison of magnitude of forces responsible for insulator contamination (particle size = $5 \mu\text{m}$). [Guror]

NaCl contamination is a problem for insulators close to the coast and is highly soluble. Gypsum (CaSO_4) is another common contaminant for inland insulators, and has a low solubility. Sand (SiO_2) acts as a non-soluble binding agent for the pollution. In agricultural areas, phosphates and nitrates of nitrogen and ammonia are commonly noticed on insulators.

2.2.2 Insulator wetting

The following wetting processes can be identified:

Rain and spray

Water particles impinging on the surface of the insulator wet the exposed sections of the insulator. Torrential rain or rain of long duration could wet the entire insulator. Such wetting could lower the resistance of the pollution layer. Heavy rain could also clean the insulator.

Dew and fog:

Wetting in this case is by the processes of condensation and depends on the temperature difference between the insulator and the ambient. Condensation wetting is characterised by a uniform distribution of tiny water droplets. Water vapour condenses on the insulator surface while

its temperature is below that of ambient. Wind assisted spray wetting can produce a pattern similar to condensation wetting, depending on the wind speed. Condensation wetting is more severe from a pollution point of view as the insulator is wetted more uniformly.

The insulator material determines the extent of wetting of the insulators in the field. Porcelain and glass insulators are hydrophilic as water adheres to the surface. Silicone rubber insulators, on the other hand, are hydrophobic.

The solubility of the contaminant also plays an important role in the insulator flashover phenomenon. Among all the salts, NaCl is the most readily soluble salt, but is not the most frequently encountered contaminant (except near the coast). Hence this salt can be expected to provide the highest leakage current. Gypsum and sand are insoluble, and other salts, which are more likely to be observed on insulators, are soluble to different degrees.

2.2.3 Dry band arcing

Leakage current causes heating of the electrolytic layer and the wet pollution layer dries out in the narrow portions such as near the pin of porcelain and glass insulators, and on the shank of composite insulators. Dry bands form in these regions and the voltage distribution along the insulator is changed significantly. As the largest portion of the applied voltage appears across the dry band, the withstand value of the gap is exceeded and arcs occur across the dry band as shown in Figure 2.4.

The dry band arcs are usually self-limiting because of the large surface resistance. However, when heavy wetting significantly reduces the high levels of contamination, the dry band can elongate sufficiently to bridge the insulator terminals, causing a flashover.

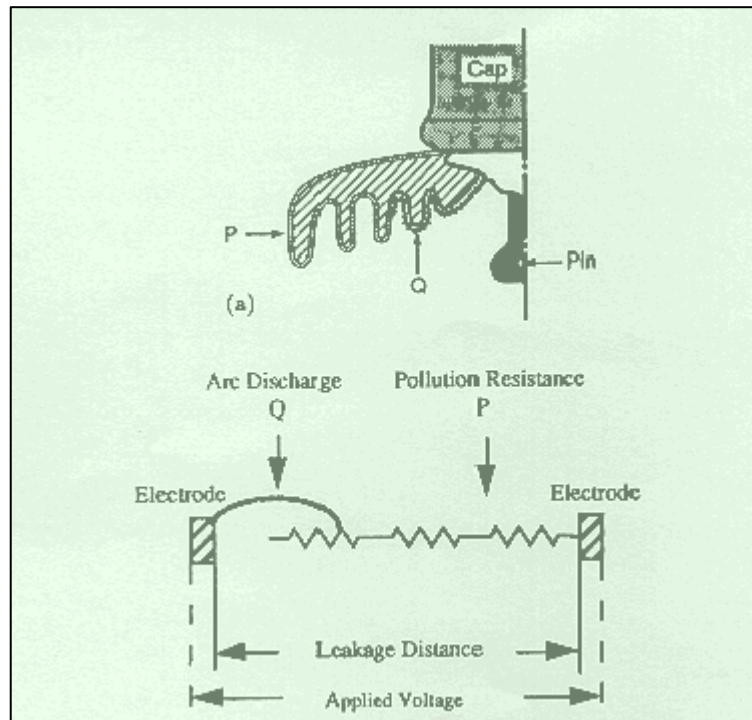


Fig. 2.4: Schematic of dry band arcing on a polluted insulator [Guror]

The processes leading to flashover are complex and depend on factors such as the uniformity of the pollution distribution. There is however consensus that flashover can be expected when the dry band arc covers $\frac{2}{3}$ of the insulator length.

Pollution flashover is also accompanied by appreciable leakage current. Verma postulated that, if this current approaches a current I_{\max} , flashover is imminent. I_{\max} is given in the following formula:

$$I_{\max} = \left(\frac{15,32}{mm/kV} \right)^2$$

where mm/kV is the specific creepage.

2.2.4 Insulator pollution severity

For the purposes of standardisation, four levels of pollution severity are qualitatively defined in IEC60815, from light pollution to very heavy pollution. According to Table 2.2, heavy pollution occurs in areas with high density of industries and suburbs of large cities with high density of heating plants producing pollution, as well as areas close to or exposed to relatively strong winds from the sea. The specific creepage distance in such areas is recommended to be 25 - 32mm/kV.

Also shown in this table are the recommended specific creepage lengths for each severity. If insulators with a specific creepage length less than recommended for a specific area are used, then an unsatisfactory pollution performance can be expected.

Pollution level	Examples of typical environments	Recommended spec. creepage
1. Light	<ul style="list-style-type: none"> • Areas with no industries and with a low density of houses equipped with heating plants • Areas with a low density of industries or houses but which are subject to frequent winds and/or rainfall • Agricultural areas • Mountainous areas <p>All these areas are situated far from the sea (10 to 20 km) and are not exposed to winds from the sea.</p>	16mm/kV
2. Medium	<ul style="list-style-type: none"> • Areas with industries not producing particularly polluting smokes and/or with an average density of houses equipped with heating plants • Areas with a high density of houses and/or industries but which are subject to frequent clean winds and/or rainfall • Areas exposed to wind from the sea but not too 	20mm/kV

	close to the coast (at least a few km)	
3. Heavy	<ul style="list-style-type: none"> • Areas with a high density of industries, and suburbs of large cities with a high density of heating plants producing pollution • Areas close to the sea or at least exposed to relatively strong winds from the sea 	25mm/kV
4. Very heavy	<ul style="list-style-type: none"> • Areas generally of moderate extension, subject to conductive dusts and to industrial smoke producing particularly thick conductive deposits • Areas generally of moderate extension, very close to the coast and exposed to sea spray or to very strong and pollution winds from the sea • Desert areas with no rain for long periods, exposed to strong winds carrying sand and salt, and subject to regular condensation 	31mm/kV

Table 2.2: Pollution levels and typical environments [IEC60815]

Under heavy pollution, uniformly distributed, the voltage distribution approaches perfection and each insulator tends to share the heavier power loss as well as the voltage applied. Eventual failure on a thermal premise usually follows.

2.3 Bird streamer flashovers

A probable cause for some unexplained transmission line outages could be because of bird streamer flashover [Burger]. It was demonstrated then that an isolated stream of bird contamination could bridge HV insulation and cause an outage without obvious evidence. This phenomenon is seldom witnessed because they occur at night in remote areas and leave little or no evidence, thus not generally accepted to constitute a significant portion of outages [West 1971].

Several bird types, including eagles, vultures and herons were considered in these tests, after consultations with experts in the field of avian physiology. These birds can release up to 60cm³ of excrement that could initiate flashover. The birds are usually driven from high mountains to lower flatlands by bad weather and low temperatures, where they roost on any high objects, such as transmission lines.

Similarities between the characteristics associated with streamer outages exist between American lines and local lines [Burnham]. With this evidence it can thus be concluded that birds may well be a cause of the unexplained outages on some of the transmission lines in South Africa [Taylor].

2.4 Fire induced flashovers

Another probable cause for some unexplained outages could be because of those conditions induced by fire [West 1979]. Occasionally it has been observed on long HV lines that a fault may occur on a warm, clear day without auto-reclosure difficulty. Such unexplained outage conditions fit those of burning field weeds, sugar cane fires, or a large rubbish pile beneath the lines.

Fires with high gas and particulate emissions, and fires capable of producing violent plume activity dangerously increases the probability of flashover of HV transmission lines. The possible conditions imposed by fire can make flashover a certainty when certain criteria are met: sufficient heat, large pressure drop due to plume configuration, high gas and particulate emissions, and large quantities of fire brands and debris carried in plume activity.

In South Africa, cane fires are the most prominent cause of known fire induced flashovers, but due to the good understanding between Eskom and cane farmers, forced outage situations are avoided by e.g., arranging to switch out a specific line within a specific time frame and burning the cane simultaneously in that area.

2.5 Hypothesis: Air breakdown, assisted by non-uniform light pollution along the string

In the case of the lines under investigation the occurrence of air flashover, normal pollution flashover and bird flashover is considered unlikely. This leads one to postulate a different flashover mechanism being experienced. The hypothesis considered is a combination of air breakdown, assisted by a non-uniform light pollution along the glass insulator string.

A number of studies have been published that suggests that the presence of a non-uniform pollution layer on the insulator surface may have an effect on the pollution flashover process.

Experiments [Guror 1997] conducted involving AC energised non-ceramic insulators, which showed that flashovers could occur in the field on those insulators where the wet surface resistance varies over a wide range along the insulator length. From Guror's work it was concluded that a convenient way of simulating sudden flashovers in the laboratory during a clean fog test was to use a fully contaminated insulator but with the part near the terminals wiped clean.

Rizk [Rizk and Kamel, 1981] showed that partially contaminated insulators show a reduction in the average equivalent salt deposit density (ESDD) required for flashover when compared to that of a fully contaminated insulator. He suggested that conventional clean fog testing could be complemented with sudden flashover experiments to provide a more comprehensive scenario from which to draw conclusions about the performance of the insulators.

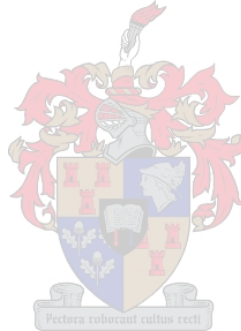
Related work was done by Rizk [Rizk, Beausèjour and Shi-Xiung, 1981] and Schneider [Schneider 1991] in connection with HVDC wall bushings. They found that the non-uniform voltage distribution along the bushing as well as within the dry zone itself constitute prerequisites for initiation of the flashover process during heavy rain.

Following on the above research, a possible sequence of events is postulated:

It is believed that a non-uniform pollution layer along an insulator string results in the highest electric field strength, and thus the highest voltage, across the cleanest / driest discs. The worst case would be when the cleanest discs were actually completely clean and dry.

The flashover across these clean discs applies the full phase voltage across the rest of the insulator string. This condition would have the same effect as the cold switch-on condition. As the insulator discs are all non-uniformly polluted, the same event could reproduce itself for the rest of the insulator string. This could result in a cascade flashover across the whole insulator string. It is postulated that breakdown could develop before the formation of dry bands.

In the following chapters a series of tests is conducted in the laboratory and in the field in order to identify conditions whereby such an anomalous flashover process is possible, if at all.



Laboratory Investigations

3.1 Introduction

In the previous chapters it was argued that a strong possibility exists that the anomalous flashovers were caused by air breakdown, promoted by the presence of conducting polluted insulator surfaces. In this chapter a series of tests is performed to investigate the likelihood of such flashovers. In these tests insulator strings similar to those employed on the problem lines were used. A number of different laboratory tests were performed in order to prove the validity of the hypothesised flashover mechanism.

3.2 The effect of pollution on the underside of the discs of a 4-disc I-string

Inspection of the insulators on the problem lines indicated that the bottoms of the glass discs were polluted while the discs were relatively clean on the top. In the tests described in this section the conductive layers on the undersides of the discs are simulated and the effect thereof on the voltage distribution, the electric field strength and flashover voltage is investigated. The test arrangement is shown in Figure 3.1.

The first step to prove the hypothesis mentioned in chapter 1 was to energise a 4-disc glass insulator string at the high voltage laboratory of the University of Stellenbosch. The glass discs used were U120BS glass insulators (see Appendix A).

3.2.1 Flashover tests

The flashover tests were done by inserting the 4-disc insulator string as a test sample, as seen in Figure 3.1. The use of a 4-disc string is because of the limitation of the voltage source of the high voltage laboratory.

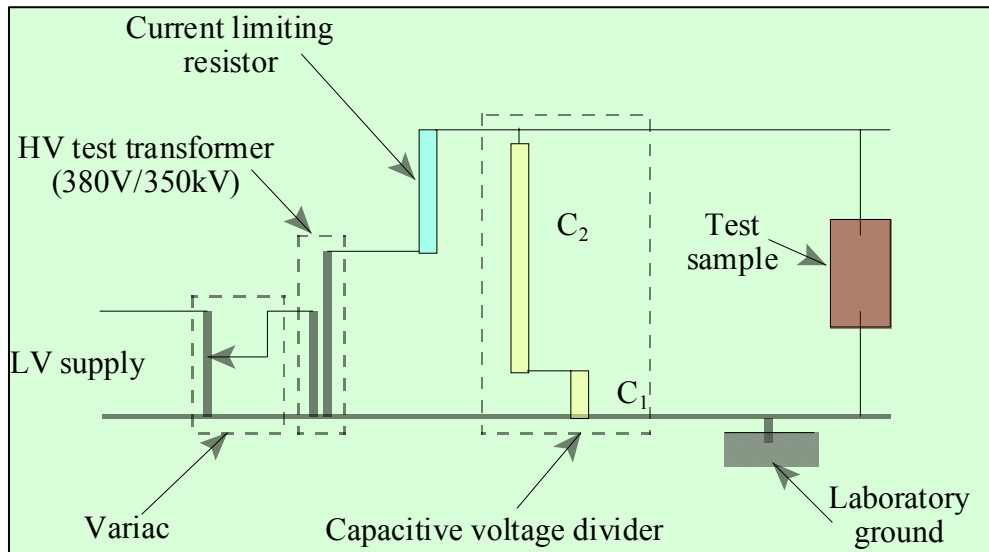


Figure 3.1: Schematic diagram showing the connection of the 350kV test transformer

The fact that the bottom sides of insulator discs are more polluted than the top of the discs, as discussed in section 1.3, was simulated by shorting out the bottom of the insulator discs using copper wire as shown in Figure 3.2. The copper wire was wound around the pin and around the outer diameter of the individual insulator. This was done for a number of discs in different positions in the string.

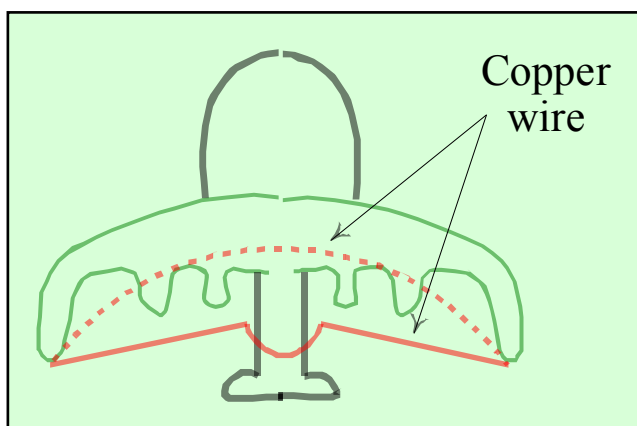


Figure 3.2: Glass insulator with copper wire wound around pin and connected to outer diameter

The voltage was then slowly increased from zero until flashover across the insulator string occurred. The voltage across the string at the instant of flashover was recorded.

The process was repeated 5 to 8 times, and the average of the values was taken. These values of the flashover voltage for different configurations can be seen in Table 3.1.

	Number of discs shorted	Position of shorted discs	Flashover voltage (kV)	% reduction in f/o voltage
1	<i>Four clean discs</i>	None	252	–
2	<i>One disc partially shorted</i>	Top	207	17.86
		Second	208	17.46
		Third	213	15.48
		Bottom	210	16.67
3	<i>Two discs partially shorted</i>	2 top	197	21.83
		2 bottom	197	21.83
		2 middle	199	21.03
		Top & bottom	196	22.22
4	<i>Three discs partially shorted</i>	Top disc not shorted	170	32.54
		2 nd disc not shorted	174	30.95
		3 rd disc not shorted	172	31.75
		Bottom disc not shorted	176	30.16
5	<i>All four discs partially shorted</i>	All discs	163	35.32

Table 3.1: Flashover voltages of 4-disc insulator string with different discs shorted underneath with copper

It will be noted that the largest reduction in flashover voltage occurs when all the four glass discs are partially “polluted”.

Discussion

In section 3.1, it was decided to perform full flashover tests on a shorter glass insulator string. This is due to the source voltage of the high voltage laboratory being just over 300kV, which was postulated to be close to the value of the flashover voltage of a clean 4-disc glass insulator string.

In Figure 3.3 the percentage reduction in flashover voltage is shown together with the percentage reduction in creepage distance and dry arcing distance (DAD) of the insulator string.

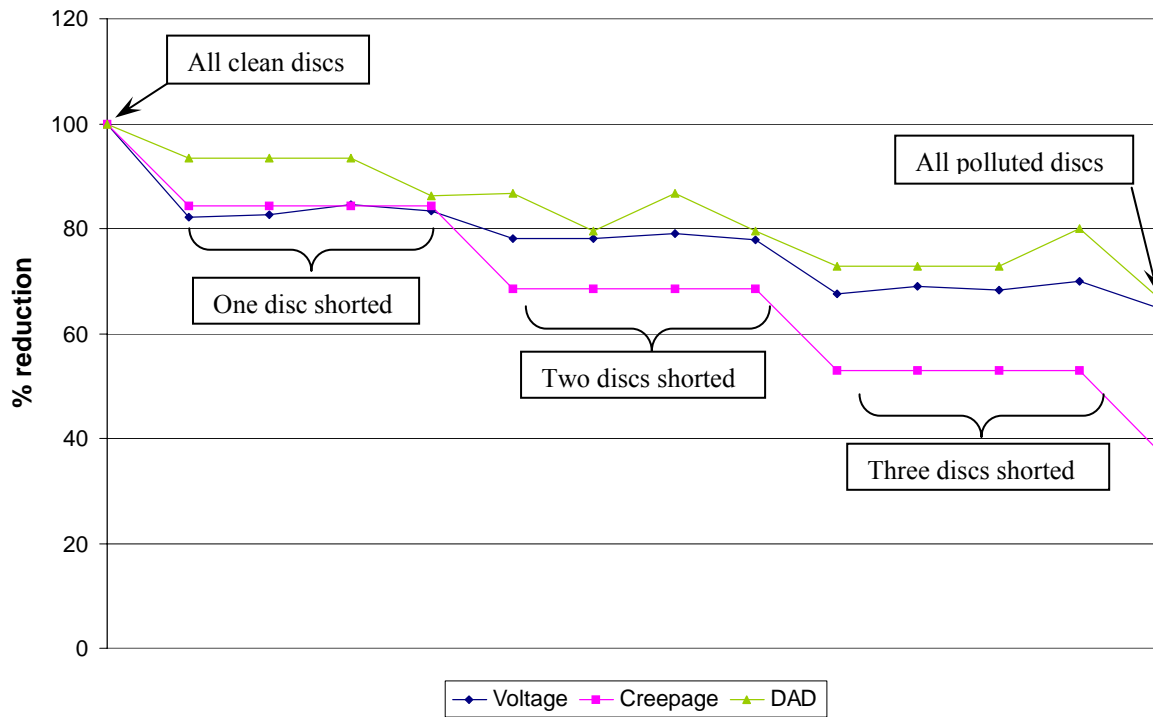


Figure 3.3: Average % reduction in creepage distance, dry arc distance (DAD) and flashover voltage for number of discs partially shorted

The dry-arc distance is defined as the shortest path through the air from the ground end to the live end. It will be noted that in the case of the partially shorted disc there is a correlation between the voltage reduction and the reduction in creepage distance.

In the case of the two and three partially shorted discs there is a correlation between the reduction in DAD and the reduction in flashover voltage.

3.2.2 Measurements taken at 50 kV: Potential and field strength distribution

In order to investigate the effect of partially polluted discs on the voltage and electric field distribution, a series of laboratory tests were done. An arbitrary voltage of 50kV AC line to ground voltage was applied across the insulator string, and the voltage was measured across each disc, as well as the electric field in the vicinity of the string.

3.2.2.1 Voltage distribution along the string

The setup used for the voltage measurement tests is as displayed in Figure 3.4.

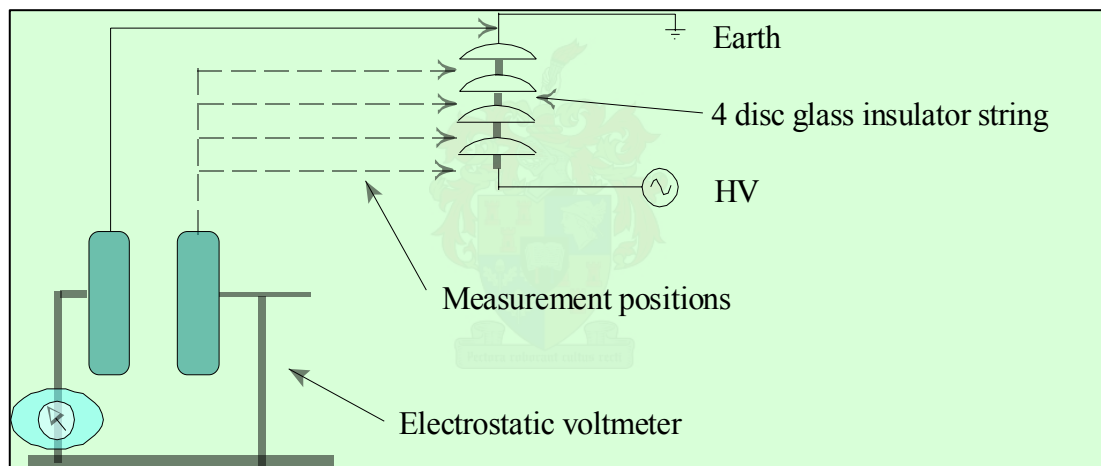


Figure 3.4: Schematic diagram of voltage measurement setup

In the above setup, an electrostatic voltmeter (ESVM) is used to measure the voltage between each of the disc positions to ground, as illustrated in Figure 3.5. An electrostatic voltmeter was used as it has a high input impedance (small capacitance) and is assumed that the voltmeter does not affect the measurement. As in the flashover tests, some of the discs were shorted underneath using two conductive agents:

- i. Aluminium foil attached underneath

Strips of aluminium foil were attached to the underside of the insulators, as was done with the copper wire in the flashover test (section 3.1.1). The results are represented in Figure 3.6 where the deviation of the measured values obtained on the “polluted” strings are given with respect to those of the string with clean discs.

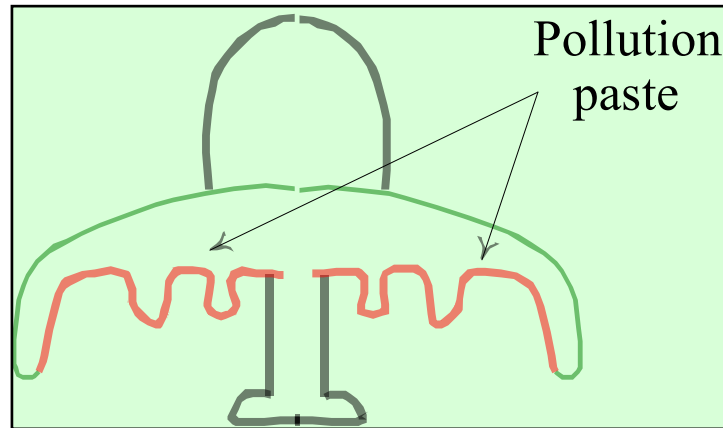


Figure 3.5: Glass insulator with pollution paste at the bottom of the disc

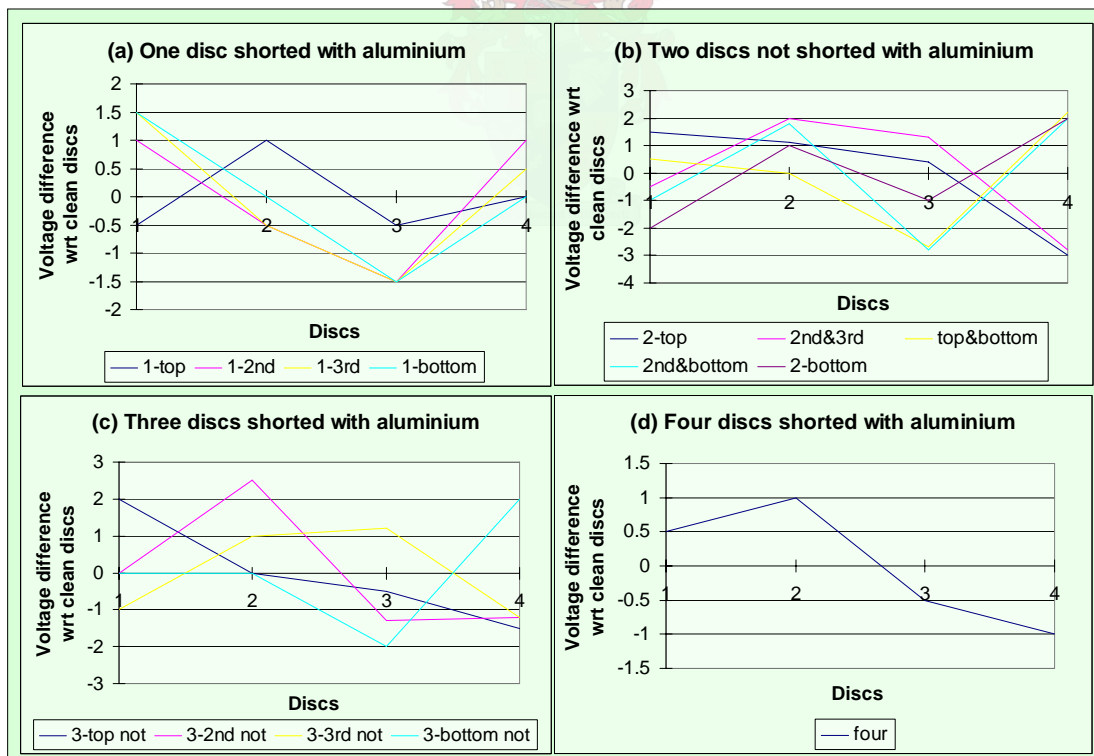


Figure 3.6: Graphs of ESVM readings with some amount of the discs shorted underneath with aluminium foil

ii. *A light-medium pollution paste applied underneath*

A paste consisting of kaolin and salt was applied to the bottom side of the discs to represent a light pollution layer. The results of the voltage measurements in the case where the paste was used are represented in Figure 3.7.

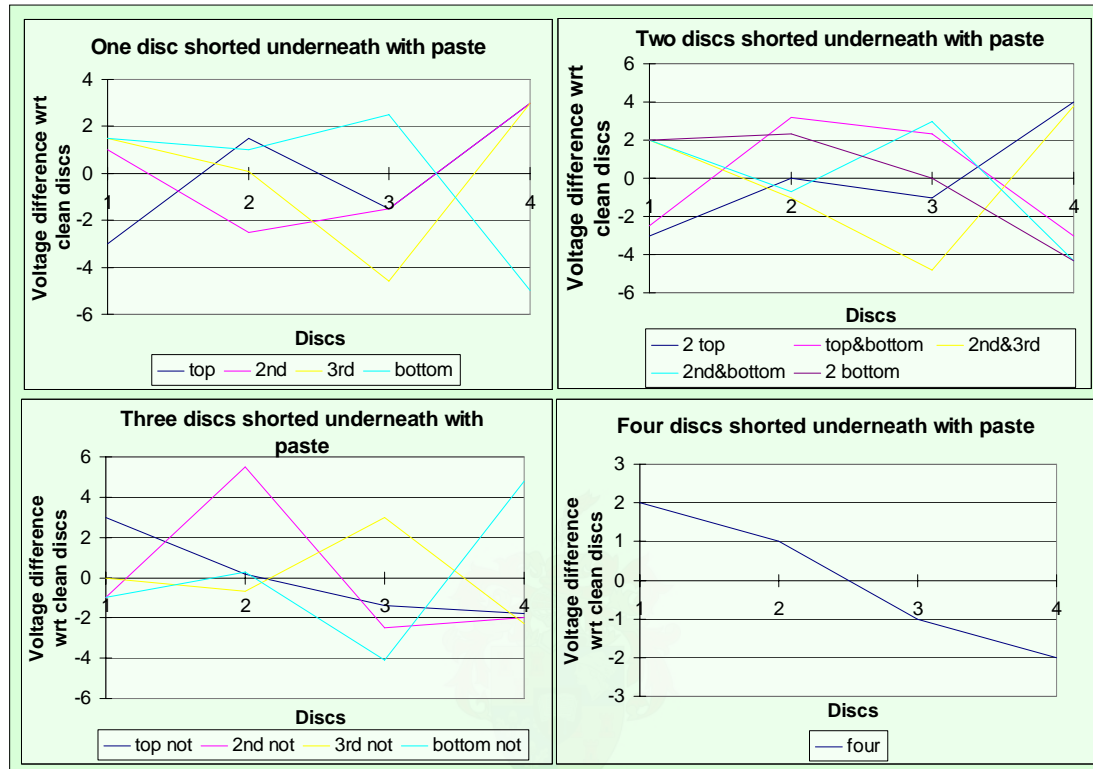


Figure 3.7: Graphs of ESVM readings with some amount of discs shorted underneath with pollution paste

Discussion

At the fixed voltage of 50kV used in the tests, a comparison could be done on the effect of different discs being polluted, as well as comparing the level of pollution used.

When specific discs in the insulator string is polluted by both types of pollutants, a change in voltage across the specific discs is observed. This change is approximately not more than 4% of the total voltage across the string, and thus not very significant in terms of this experiment. This could however be different for longer insulator strings within a tower window, due to a higher applied voltage, and different electric field

strength. With all four discs polluted, the voltage distribution has less deviation from the values of the clean insulator string, and would actually promote the chance of air flashover not occurring.

The overall trend of the tests indicates a reduction in voltage from a clean insulator string if specific glass discs are polluted. This phenomenon is seen more accurately with the results of the pollution paste tests. Moreover, when the disc closest to the live end is clean, and the adjacent discs are polluted, the ground potential is shifted and the full line current appears over this clean disc. In the above tests, this amounts to more than 50% of the applied voltage. At higher voltages this could lead to the breakdown of air and resultant localised flashover across this clean disc.

A four disc insulator string would normally operate at a line to line voltage of 44kV, i.e. a phase to neutral voltage of $\frac{44}{\sqrt{3}} = 25.4\text{kV}$. It is apparent that this voltage is much

less than the lowest flashover voltage measured, i.e. 163kV.

3.2.2.2 Electric field along the string

The electric field measurements were carried out using a spherical probe designed by D. R. Cockbaine of the University of Witwatersrand. The spherical probe measures the electric field around high voltage structures with as little perturbation of the field as possible. A remote reading AC fieldmeter was used to receive signals from the probe via an optical cable. The probe was then moved in a plane parallel to the centre axis of the insulator string. Thus, the values obtained are not the values of the electric field very close to the insulator, but the field in close proximity around it.

The setup used is shown in Figure 3.8.

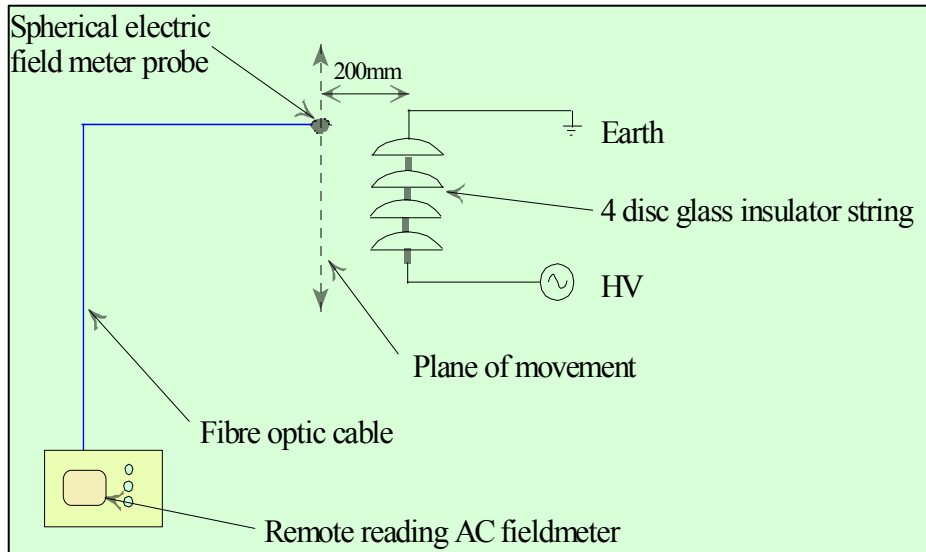


Figure 3.8: Schematic diagram of electric field measurement setup

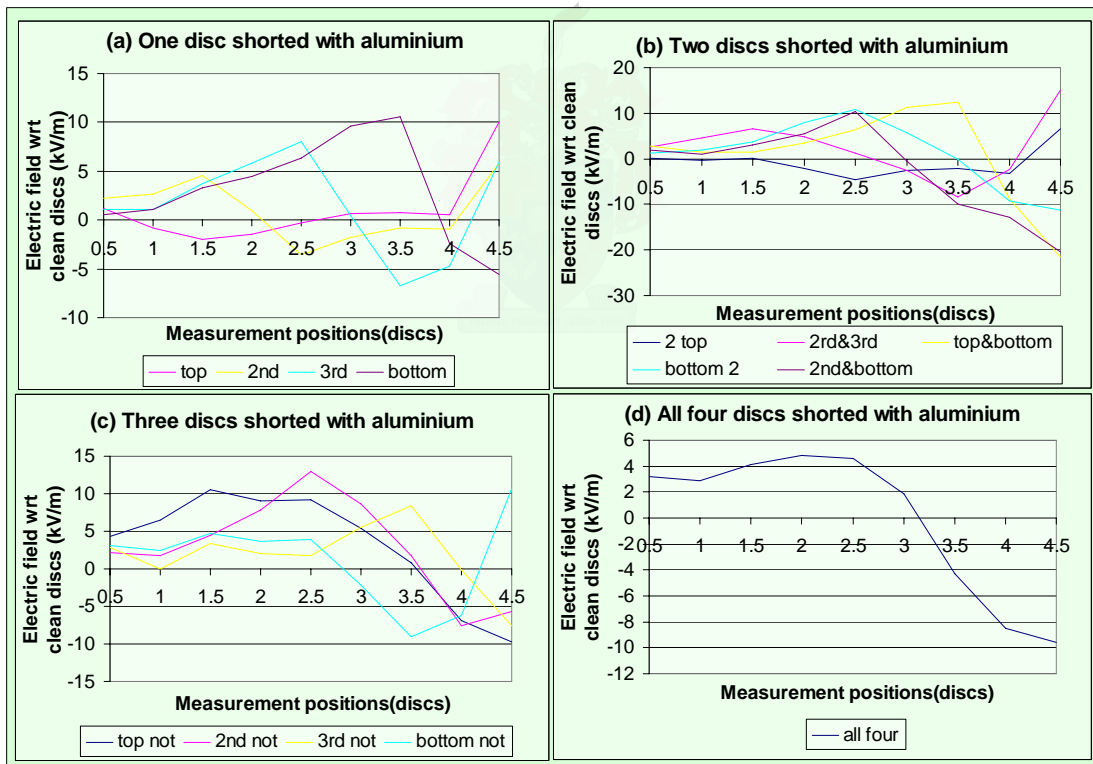


Figure 3.9: Graphs of electric field readings with some amount of discs shorted underneath with aluminium foil

As with the ESVM readings, the same readings were done with the spherical electric field probe, in order to establish whether there is any difference in the

electric field of a clean insulator string and polluted ones. Graphs for the electric field using aluminium foil as a conductive agent is illustrated in Figure 3.9, and pollution paste is shown in Figure 3.10.

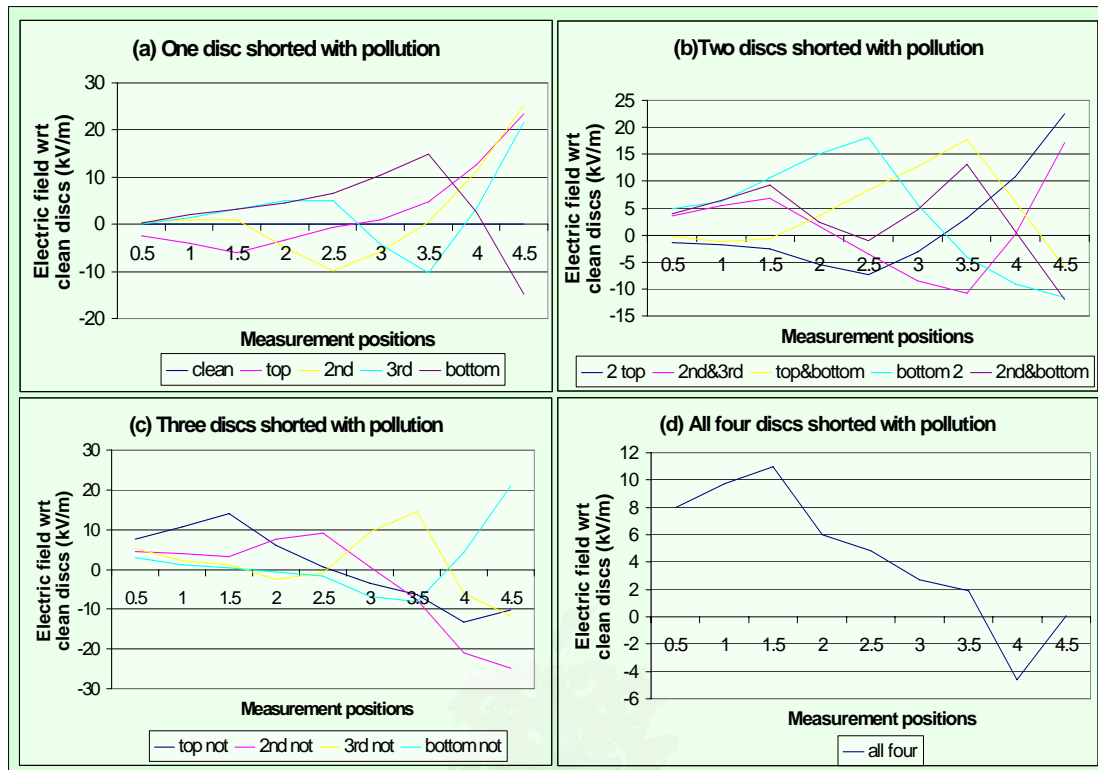


Figure 3.10: Graphs of electric field readings with some amount of discs shorted underneath with pollution paste

Discussion

With one disc shorted, the reduction in field strength across polluted discs is $\pm 33\%$, and the increase in field strength over the clean disc is $\pm 17\%$. The tests performed with two discs shorted indicates a reduction of $\pm 66\%$ in field strength across discs with pollution present, and an increase across the clean discs of $\pm 33\%$. Having three discs shorted produced reduction of $\pm 33\%$ across polluted insulators, and an increase of $\pm 33\%$ across the clean discs is observed. With all four discs polluted, the field strength distribution has less deviation from the values of the clean insulator string.

The above results also show a similar trend as with the tests performed with the voltmeter. The highest electric field strength is situated across clean discs that are adjacent to polluted discs. The actual values (maximum value of $2,8\text{kV/cm}$) are still

much less than the breakdown of air (10kV/cm). This however confirms that at higher voltages this could lead to the breakdown of air and resultant localised flashover across these clean discs.

3.2.2.3 Electric field inside fog chamber

It was decided to use the same setup for the electric field measurements in the fog chamber of the University of Stellenbosch. The fog chamber has a rating of 22kV rms, but it has a stronger source. Flashover was still very unlikely, even under 100% relative humidity. The setup used is shown in Figure 3.11.

The spherical probe was protected from excessive exposure to humidity by covering it with a Latex covering, which would keep it water tight, yet have no adverse effect on the electric field measurements.

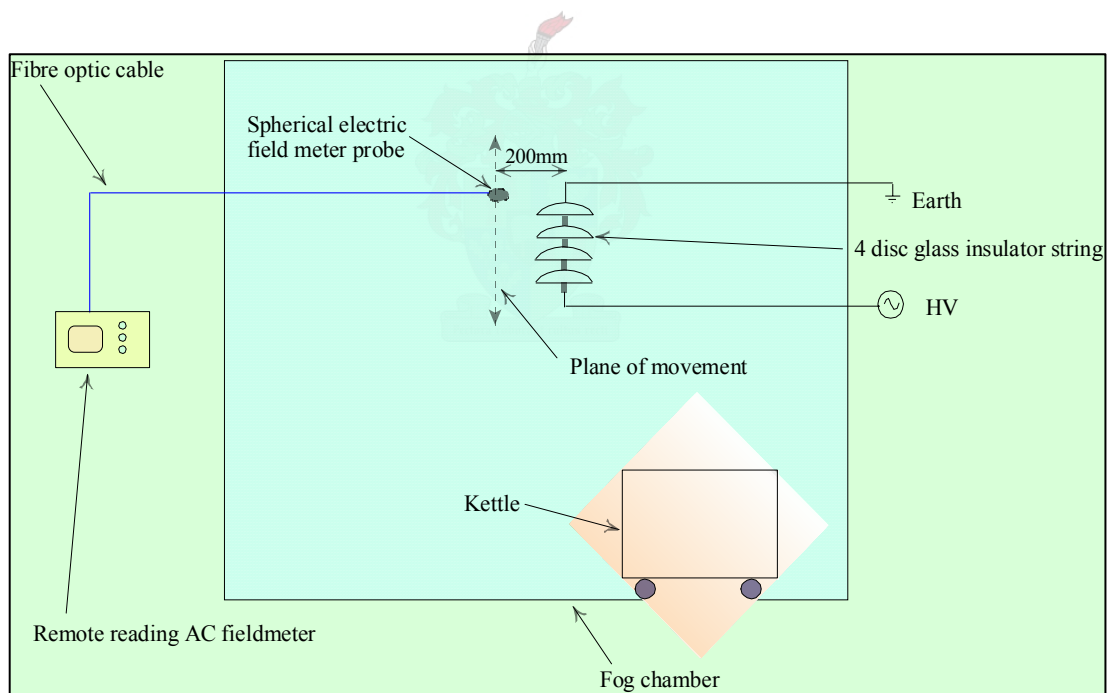


Figure 3.11: Schematic diagram of fog chamber setup

The humidity inside the fog chamber caused excessive condensation on the surface of the spherical probe. This distorted the electric field in the immediate vicinity of the probe, and thus caused erratic value fluctuations. Due to the sensitivity of the electric field probe, no accurate and coherent readings could be taken of the electric field strength.

3.3 The effect of two clean discs in a lightly-polluted 16-disc I-string

The next logical step was to investigate the effect of a non-uniform distribution of a conductive surface layer along the length of a 275 kV cap and pin insulator string [Kleinhans 1999]. The worst case is when one or two clean discs are inserted in a polluted string. The electric field and the actual voltage distribution are measured to compare a polluted string with a clean string. The test environment used is the same as in Figure 3.1.

3.3.1 Laboratory tests

For the following experiments, the test procedures were as follows:

- A test transformer, rated at 350kV, was used. It had high source impedance, and therefore did not comply with the source requirements for pollution tests. The object of these tests, however was not to do pollution tests, but to investigate the voltage and electric field distribution along the length of the insulator string.
- The type of insulator used in these experiments was the U120BS cap and pin insulator string.
- Two clean insulator discs were inserted in three different positions in the insulator string: at the top, in the middle and at the bottom of the string. This was done to see whether the positioning of the clean discs in the insulator string held any significance with respect to the flashover voltage, as well as the voltage and electric field distribution along the insulator string.
- For these tests, two types of conducting layer were used as before to simulate the effect of the conductivity of the layer on the process:
 1. Aluminium foil (which effectively meant that the rest of the string was shorted out).
 2. A light pollution solution, which was sprayed onto the glass surface of the insulators. The light pollution solution had an ESDD of 0.05 mg/cm^2 .

3.3.1.1 Flashover tests

For the flashover tests, the supply voltage was slowly increased until local flashover occurred across the two clean discs.

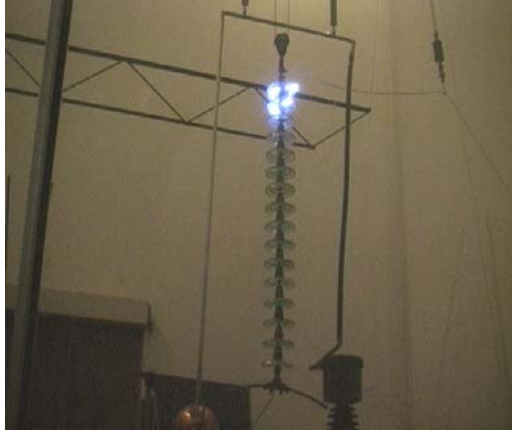


Figure 3.12: Local flashover across the two clean discs at the dead end.



Figure 3.13: Local flashover across the two clean discs in the middle



Figure 3.14: Local flashover across the two clean discs at the live end.

In Figure 3.12, the two clean discs were situated at the dead end (top) of the insulator string, in Figure 3.13 the discs were moved to the middle of the string, and in Figure 3.14 it was inserted at the live end (bottom) of the insulator string.

The three pictures shown above only illustrated the effect of the light pollution layer that was sprayed on. In all three cases, though, the corona onset voltage

was 80kV, and localised flashover across the two clean discs occurred at 130kV, irrespective of the positioning of the two clean discs in the insulator string or the type of conductive layer used.

The above results could be extrapolated to natural conditions, where two discs in a polluted 275kV glass insulator string is clean, or dry. These tests did not lead to a flashover of the entire string, and thus could not on its own be the cause of the anomalous flashover phenomenon.

3.3.1.2 Voltage and electric field measurements

For these tests the supply voltage was kept constant at an arbitrary voltage of 50 kV, and the following measurements were done:

- i. The voltage across the insulator string was measured using an electrostatic voltmeter, having an input capacitance that was considered negligible compared to that of a single disc. The setup for this test is illustrated in Figure 3.15.

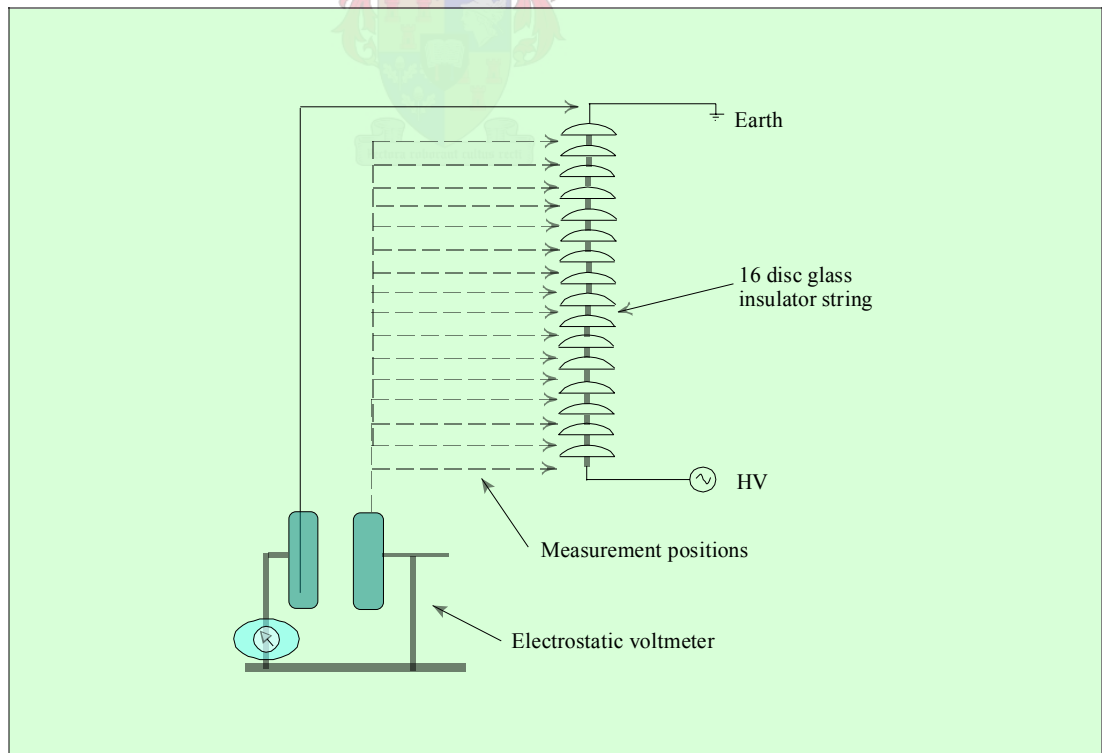


Figure 3.15: Schematic diagram of voltage measurement along insulator string

- ii. At constant supply voltage, the electric field was measured along a line, parallel to and separated 200mm from the axis of the insulator string. Measurements were done using a spherical probe, having a diameter of 50mm. The setup for this test is illustrated in Figure 3.16.

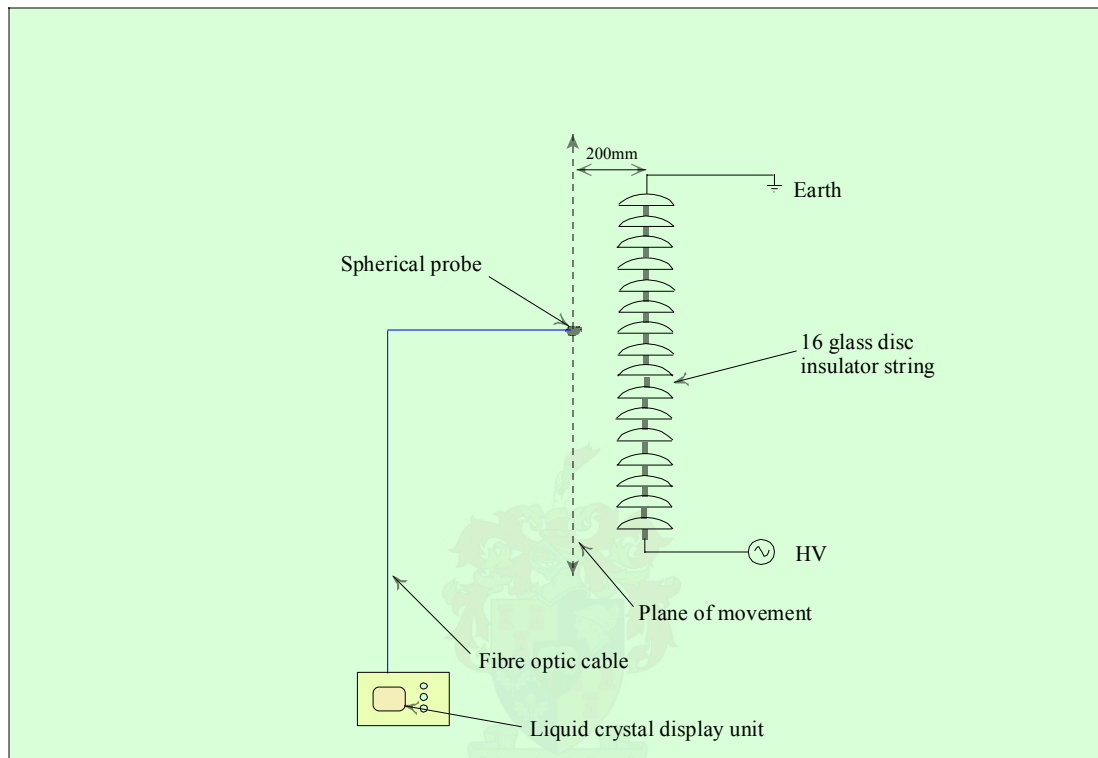


Figure 3.16: Schematic diagram of voltage measurement along insulator string

As for the flashover tests, two types of conducting layer were used (aluminium and light pollution solution) to simulate the effect of the conductivity of the layer. The calculated values for the voltage distribution across a clean glass insulator string used in these results was done using the formula described in section 2.1 for a 16-discs string.

From these test setups the following results were obtained:

- a. For the two clean discs inserted at the dead end (top), the voltage and electric field measurements are shown in Figures 3.17 and 3.18.

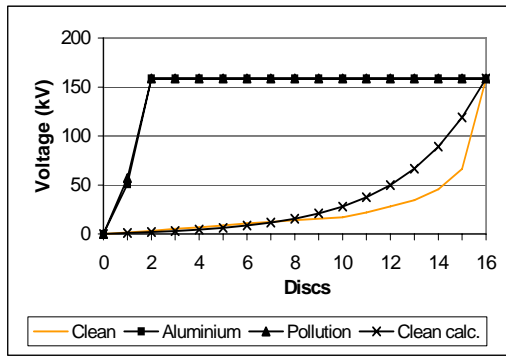


Figure 3.17: Voltage distribution over the insulator string with the clean discs at the dead end (disc 1 is at the dead end)

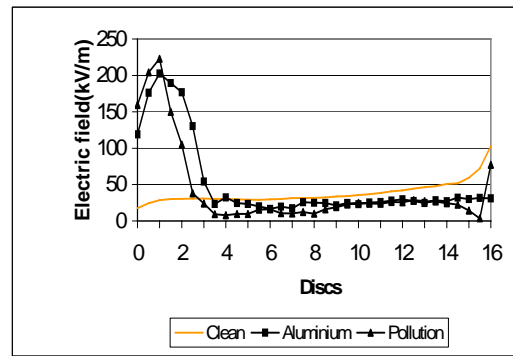


Figure 3.18: Electric field along the insulator string with the clean discs at the dead end (disc 1 is at the dead end)

- b. Next, the two clean insulator discs were shifted from the grounded end to the middle of the insulator string. Here, too, the voltage to ground across each insulator was measured, as well as the electric field strength around the string. These are illustrated by Figures 3.19 and 3.20.

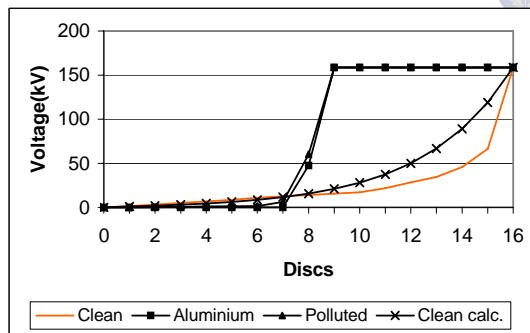


Figure 3.19: Voltage distribution over the insulator string with the clean discs in the middle (disc 1 is at the dead end)

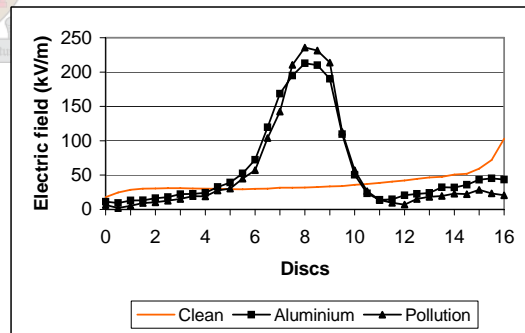


Figure 3.20: Electric field along the insulator string with the clean discs in the middle (disc 1 is at the dead end)

- c. For the next set of tests in this experiment, the clean insulators were placed at the high voltage side of the insulator string, simulating the clean discs at the bottom or “live end” of the string. Again voltage and electric field

measurements were obtained. These results were obtained and are shown in Figures 3.21 and 3.22.

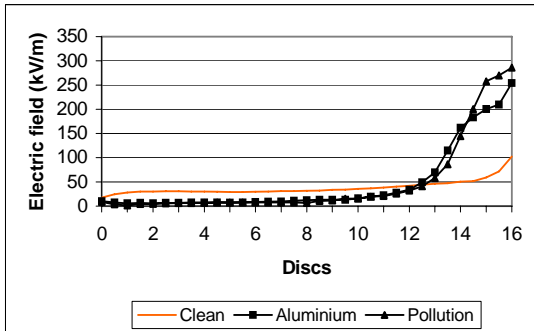


Figure 3.21: Voltage distribution over the insulator string with the clean discs at the live end of the insulator string (disc 1 is at the dead end)

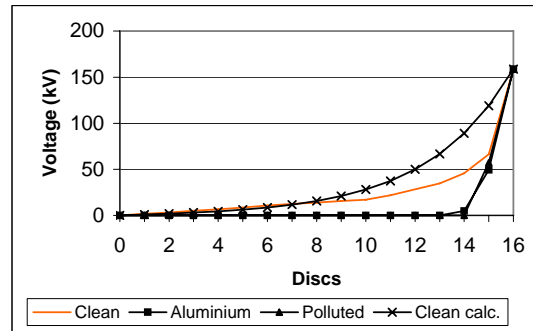
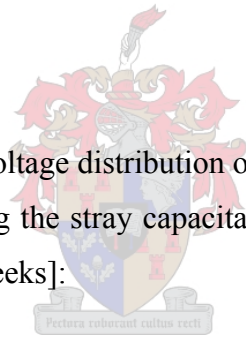


Figure 3.22: Electric field along the insulator string with the clean disc at the live end of the insulator string (disc 1 is at the dead end)

Discussion

As mentioned in chapter 2, the voltage distribution over a clean 16-disc glass insulator string can be calculated, ignoring the stray capacitance to the conductor and ground, using the following equation [Weeks]:



$$V_n = V_0 [\sinh(\alpha n)] / [\sinh(16\alpha)] \quad (1)$$

In the above formula,

n = unit number

V_n = voltage across n units from the ground end

V_0 = voltage across all 16 units

$\alpha = \sqrt{c/C}$

c = capacitance of one unit to ground ≈ 2.2 pF

C = capacitance between cap and pin. ≈ 30 pF

However, using Figure 3.12 with the two clean discs inserted at the grounded end, an equivalent of the circuit in the form of a circuit diagram is shown in Figure 3.23.

In Figure 3.23 all stray capacitances to ground as well as the surroundings are not shown. For a clean glass insulator disc, however, the capacitive impedance is the dominant value in the total impedance of the disc. The resistances are due to the pollution layer on the insulator surfaces. Since R in Figure 3.23 is very low relative to Z_C , almost all the applied voltage is across the clean discs, and thus localised flashover over the two clean discs is expected.

The measured voltage and electric field distribution across the 16-disc insulator string clearly indicates that field enhancement occurs across the two clean discs. This is to be expected as the pollution layer in fact “applies” the full voltage across the two clean discs. In each of the three cases considered, the flashover voltage across the two discs is 159 kV. As the dry power frequency flashover voltage of a single disc of the type used here is 72 kV, it is obvious that the two discs will flash over. This was

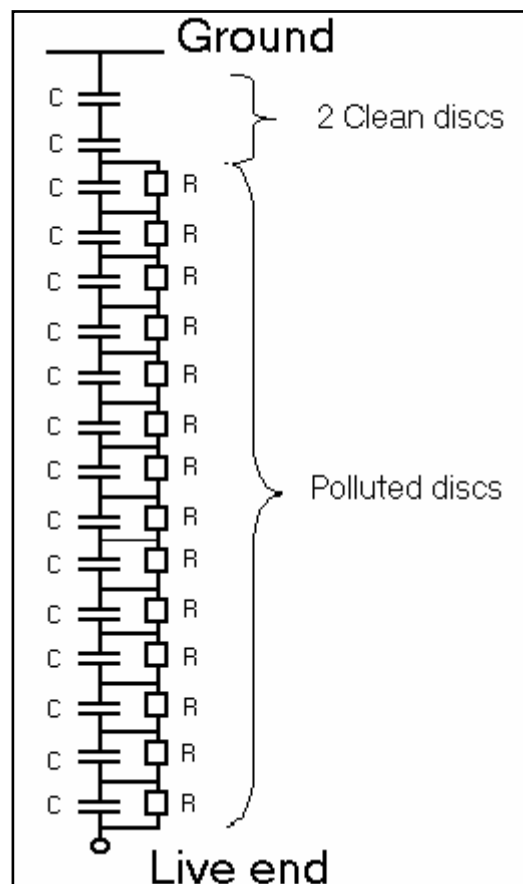


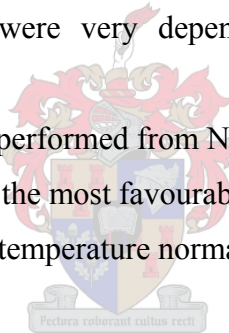
Figure 3.23: Equivalent diagram for 16-disc insulator string with the clean discs at the ground end

confirmed by the partial flashover tests shown in Figures 3.12, 3.13 and 3.14. These tests also confirm that the value of the conductivity of the pollution layer has little effect on the voltage and electric field distribution.

3.3.2 Night tests to investigate heating of discs adjacent to the current carrying conductor

From discussions in chapter 1, it can be seen that most of the unknown flashovers occur at night. The atmospheric conditions prevalent during the times of these unknown or spurious flashovers are those associated with temperatures close to dew point together with a relative humidity of greater than 75% [Britten 1999]. From this observation, tests would have to be done from sunset until sunrise the next morning, in open-air conditions, to determine the effect of temperature and atmospheric conditions on the glass insulator string. This would also mean that the tests were very dependent on favourable atmospheric conditions.

All the following tests were performed from November 1999 to April 2000. This period in the year allows for the most favourable conditions to perform these experiments, as the ambient temperature normally reaches a value close to dew point temperature.



3.3.2.1 The influence of conductor temperature on insulator performance

The maximum permissible temperature of conductors is that which results in the greatest permissible sag, or that which results in the maximum allowable loss of tensile strength by annealing throughout the life of the conductor. The conductor temperature will depend on the load current, the electrical characteristics of the conductor, and the atmospheric parameters such as the wind and sun. The conductor subsequently heats the surrounding air and may thus also raise the temperature of the adjacent discs.

3.3.2.1.1 Temperature measurements on an unenergised string

In order to simulate the effect of temperature only on an insulator string, it was decided to use a heating element inside a bundle conductor. A light pollution solution [IEC-60815] was pre-deposited on the insulator string, and allowed to dry to obtain the effect of ambient temperature on the insulator string, if any.

The element was controlled in such a way so as to keep the temperature of the conductor at a constant value. A 16-disc glass insulator string was used in the tests, which is the exact length of an insulator string used in the field. Temperature measurements were done using a handheld temperature sensor measuring the surface of an object. Measurements were done starting from the bottom of the string, measuring the pin, glass surface and cap of each insulator disc. A reading of the clamp temperature was also done in each case.

The experimental setup is shown in Figure 3.24.

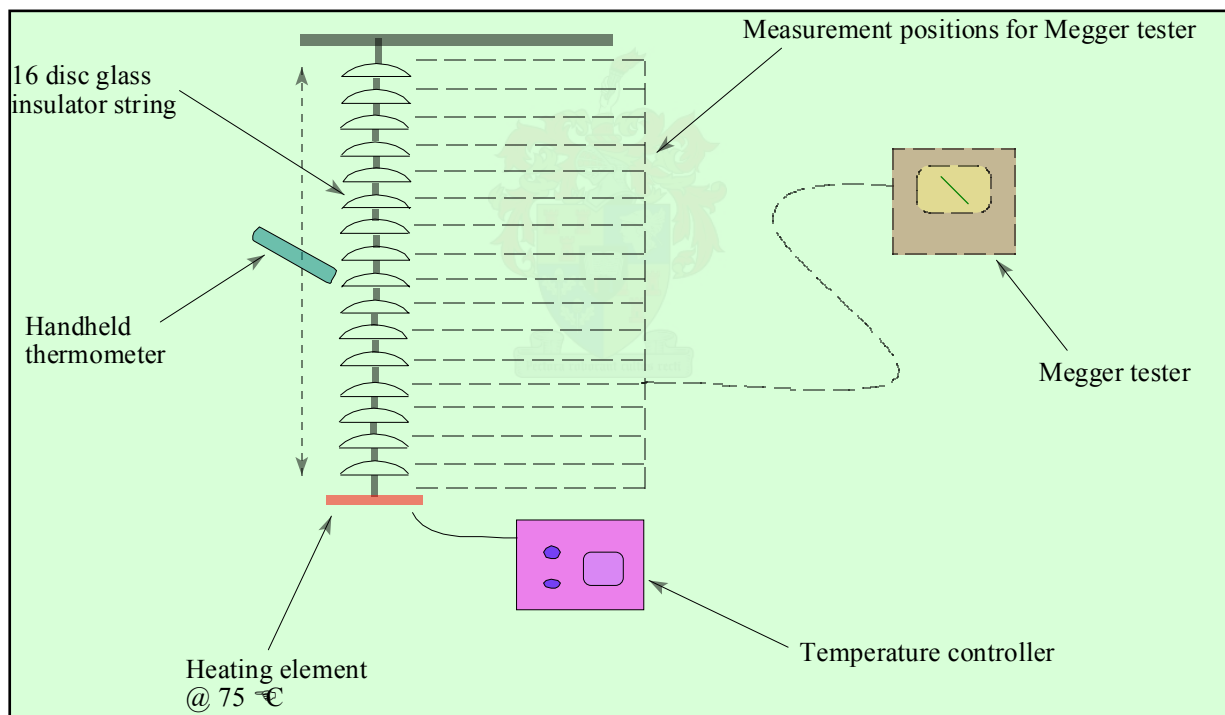


Figure 3.24: Experimental setup of temperature and resistance readings

Hourly measurements were taken from sunset until sunrise the next morning to ascertain the effect of conductor heating on the glass insulator string. Two temperatures were used being 60°C and 75°C. The significance of 75°C is due

to it being used as the first temperature threshold of a conductor, whereas 60°C is the temperature of the conductor rated at maximum load.

The results of the tests are shown in Figures 3.25 and 3.26.

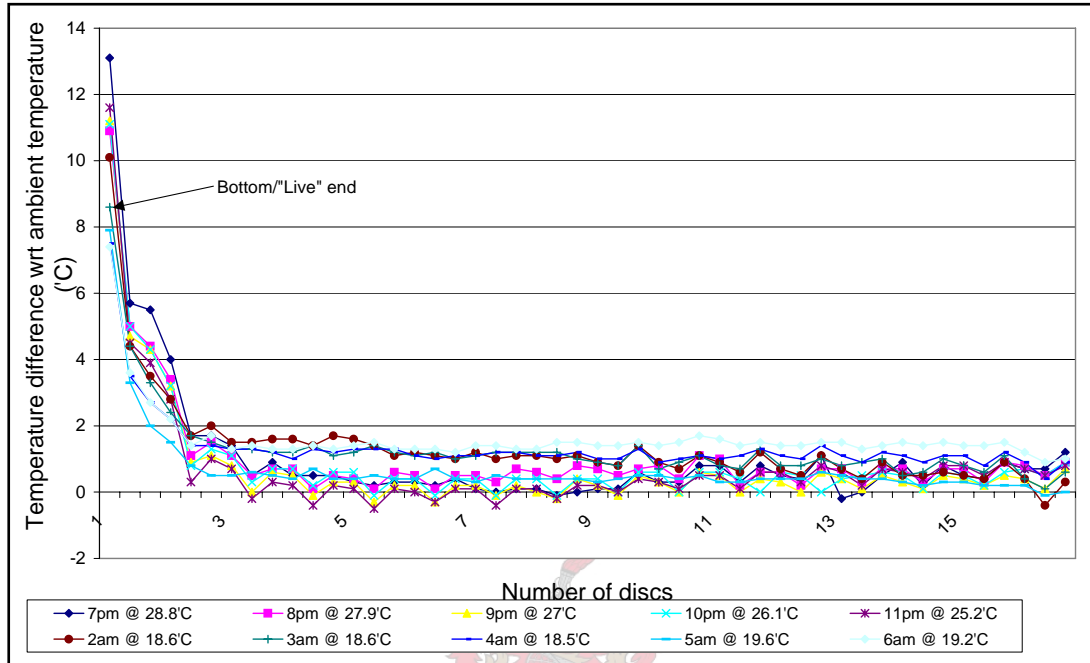


Figure 3.25: Temperature readings with conductor at 75°C

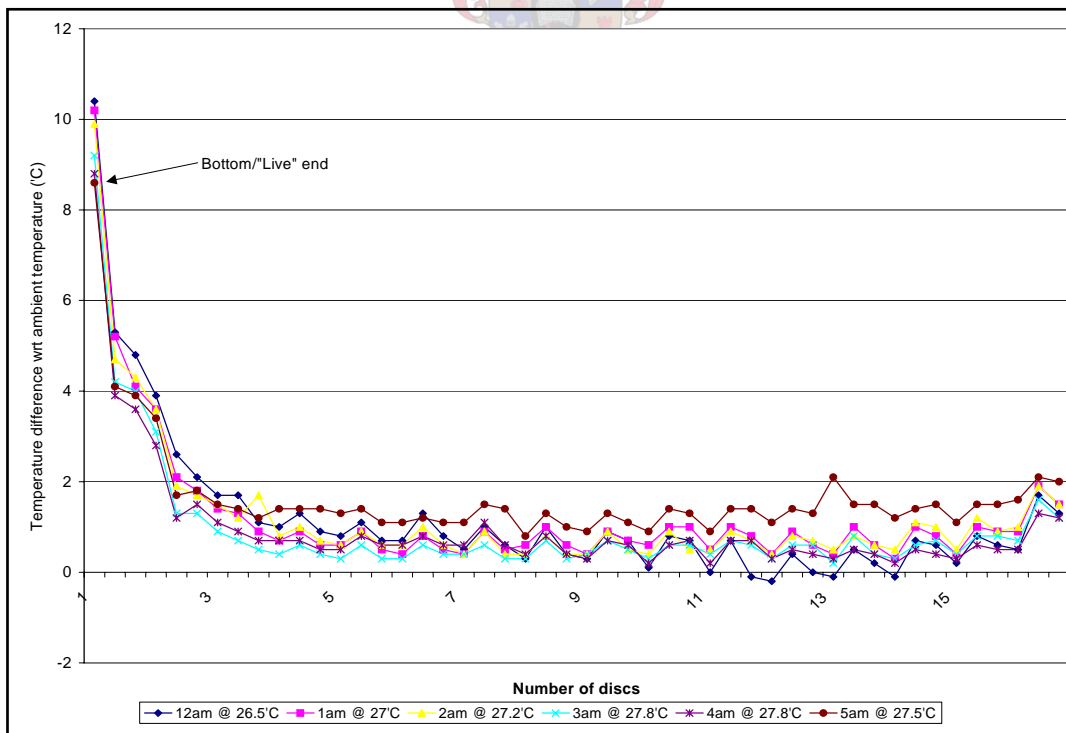


Figure 3.26: Temperature readings with conductor at 60°C

3.3.2.1.2 Resistance measurements across string

Resistance measurements were taken concurrently with the temperature readings, as illustrated in Figure 3.24. These measurements were taken using a Megger and measuring across the individual glass discs in the insulator string. The results of the measurements are shown in Figure 3.27.

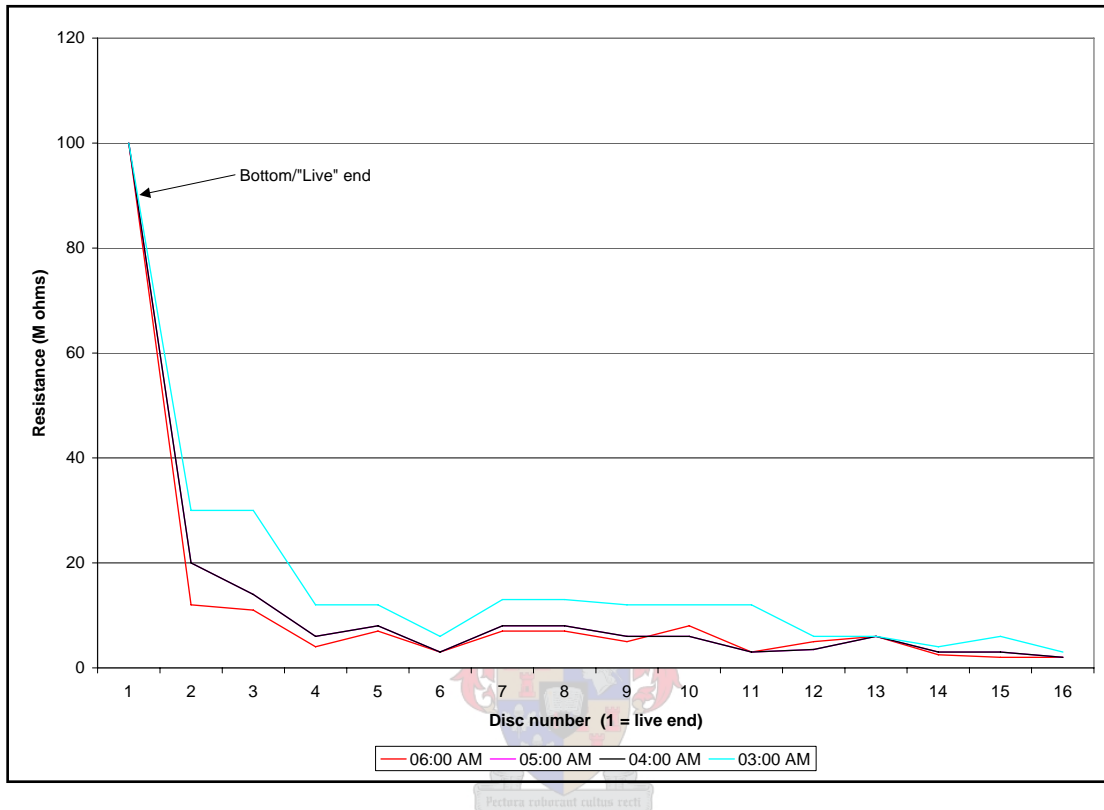


Figure 3.27: Resistance measurements with conductor at 75°C

Discussion

The results indicate a large temperature and resistance increase in the region of the “live end” of the insulator string. At the live end disc, the pin is 8 – 13°C higher than the ambient temperature, and the glass surface of this disc is 4 – 6°C higher. The rest of the string has a temperature of $\pm 1.5^\circ\text{C}$ from the ambient value.

The resistance at the “live end” disc of the insulator string has a value of $\approx 100\text{M}\Omega$. As a glass disc has a capacitance value of 30pF (chapter 2), and Z for a clean disc is

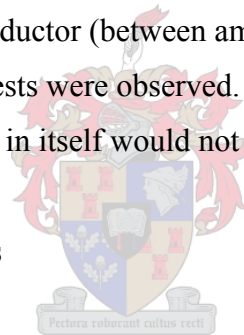
$$Z = \frac{1}{\omega C} = \frac{1}{2\pi f (30 \times 10^{-12})} \approx 106\text{M}\Omega,$$

this “live end” disc has a resistance approximately equal to that of a clean glass disc. This is significant, as the second disc from the “live end” has a value of 10 – 30M Ω , and the rest of the discs in the string have a value of less than 10M Ω . This is due to the fact that during the night, when the ambient temperature reaches dew point temperature, water condenses on the surfaces of the glass discs. The surface of the “live end” discs however is at a temperature higher than that of ambient, and thus it stays dry. The resistance of the rest of the insulator string is thus much lower due to the wetting of the light pollution layer on the glass discs.

If these values are extrapolated to the tests done in section 3.2.1, it could be postulated that when a voltage is applied to the conductor, taking only temperature into account, the line to ground voltage would be over the “live end” disc causing, as seen in section 3.2.1, a localised flashover.

At lower temperatures of the conductor (between ambient and $\pm 50^{\circ}\text{C}$) no temperature differences as seen from above tests were observed. Thus at normal operating conditions the above phenomena in itself would not cause an anomalous flashover.

3.4 The effect of V-strings



Continuing from the previous section similar tests were done on V-string insulators. These tests were done due to the fact that the “rogue flashover” phenomenon occurred predominantly on the centre phase V-string insulators.

Firstly, tests were conducted on a set of 25kV traction insulators. Pollution was pre-deposited on the surface, then the pollution was non-uniformly applied, and finally the insulators were placed in a dry-ice chamber.

The next step was to observe the effect of similar conditions on a 32-disc V-string insulator.

Following these tests, the V-string was suspended from a 275kV tower to observe any further anomalies.

These results are finally analysed and discussed.

3.4.1 Tests on the 25kV traction insulators

As it was quite difficult performing tests on a 32-disc V-string insulator, it was decided to construct a small-scale model of the insulator. This was achieved by using two 25kV traction insulators, and coupling it in the shape of a typical V-string insulator, as shown in Figure 3.28 below. The caps and pins of a normal glass insulator string were simulated using copper bands.

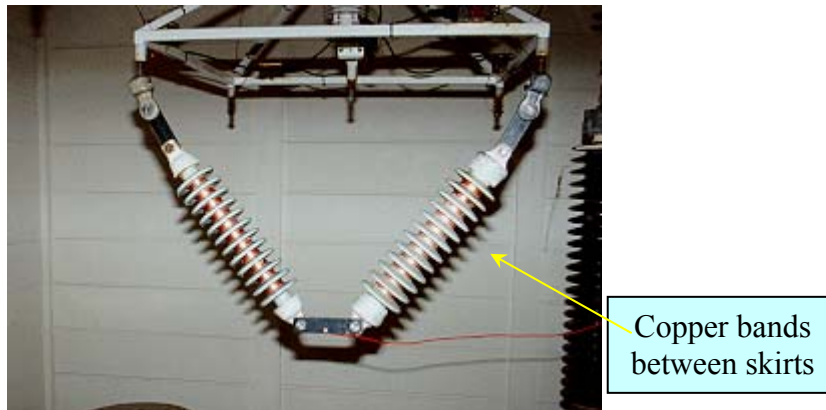


Figure 3.28: Experimental setup of the 25kV traction insulators

3.4.1.1 Pre-deposited pollution

Tests were performed in the fog chamber at the High Voltage Laboratory. During these tests a light pollution layer was sprayed on the insulator and allowed to dry. On different occasions 2 discs were cleaned and the rest left polluted. The insulators were then exposed to clean fog conditions in the fog chamber, and electric field strengths were measured via the spherical electric field probe, as well as the leakage current over the surface of the insulator.

As with the tests in section 3.1.2.3, due to the sensitivity of the electric field probe, no accurate and coherent readings could be taken. No leakage currents were also detected.

3.4.1.2 Non-uniform pollution

A wet pollutant was then applied to the insulator surface, and again 2 discs were kept clean. Once when voltage was increased, flashover was obtained. This was however an isolated incident, as the results could not be duplicated again.

3.4.1.3 Condensation using dry-ice chamber

As described earlier, a frequent sequence of events is that airborne salt is deposited on the surface of the insulator during a dry period [Looms, 1990]. It subsequently becomes wetted, thus producing a highly conducting electrolyte, which is the key component in the flashover process [Rizk, 1981].

It has been showed that moisture deposition from humidity is appreciable when the temperature of the insulator is somewhat lower than that of the ambient air, as can occur at sunrise due to the heavy thermal lag of the solid. [Orbin Swift, 1994]

The saturation temperature $T_s(K)$, or dew point, is the value at which a given mixture of water vapour and air is saturated.

Using this theory, a dry-ice chamber was constructed as shown in Figure 3.29. Dry ice was deposited at the bottom of the chamber, and air was circulated via four fans. Regular temperature readings were taken to ensure the air in the chamber was sufficiently regulated to a value well below that of the dew point temperature.

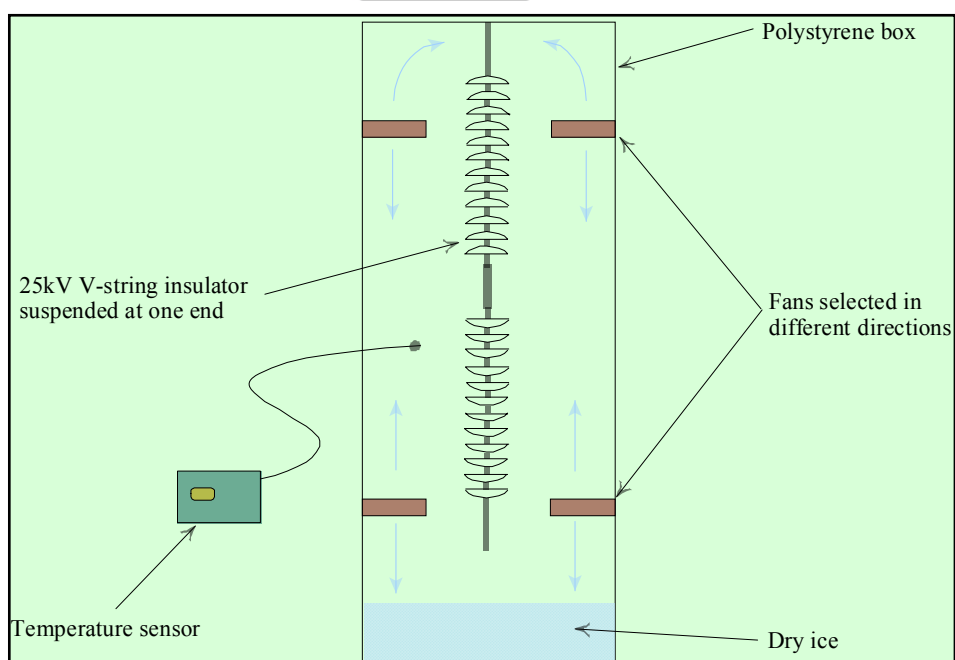


Figure 3.29: Experimental setup of the dry-ice chamber

As in section 3.3.1.1, the pollutant was sprayed on and allowed to dry. The insulators were then placed in the dry-ice chamber and cooled down until the surface temperature of the insulators were close to 0°C.

As previously done, on different occasions 2 discs were cleaned and the rest left polluted. The insulators were then exposed ambient conditions and energised at 22kV.

In all cases no leakage current were observed and no flashover occurred.

Discussion

The 25kV traction insulator has only 12 skirts, and is thus not a true scale model of the 275kV V-string insulator. It does however allow us to demonstrate the postulated effects of the hypothesis on a smaller scale, as it is not possible to do so with a 32-disc glass insulator string.

During the pre-pollution deposit tests that was done on the insulator string, as explained in section 3.1.2.3, the humidity inside the fog chamber caused excessive condensation on the surface of the spherical probe. This distorted the electric field in the immediate vicinity of the probe, and thus caused erratic value fluctuations. No electric field measurement values could therefore be taken.

As two of the “discs” were left clean, no leakage current could flow over the insulator surface. This is to be expected, as the voltage across the insulator string would be concentrated across the clean discs, and leakage current flow would only be expected if these discs were to flash over.

The wet pollutant tests were done in the High Voltage laboratory, but no positive result could be obtained.

Using the dry-ice chamber to cool the insulators down to a temperature below ambient, using the theories as in section 3.2.2, the same results were observed as in section 3.3.1.1.

The no-fog conditions gave no result due to the fact that the condensation on the insulator surface evaporated rapidly when taken out of the dry-ice box, due to a much higher ambient temperature. Due to technical and financial reasons, no bigger dry-ice box could be constructed to test the insulators on the inside.

3.4.2 Flashover tests on a 32-disc V-string

As the results of the 25kV insulators were inconclusive, it was decided to do flashover tests of the 32-disc V-string insulator in order to observe the dynamics of the arc produced during these tests. The same test procedure was used to do the flashover tests as in section 3.2, where two clean insulator discs were inserted at the top of the insulator string.

The supply voltage was then slowly increased until local flashover occurred across the two clean discs. From the resultant arc (Figures 3.30 & 3.31) it was observed how convection “pushed” the arc upwards towards the top earth plane.

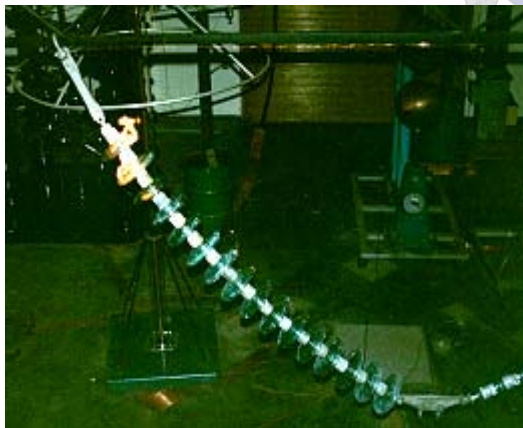


Figure 3.30: Arc initialisation

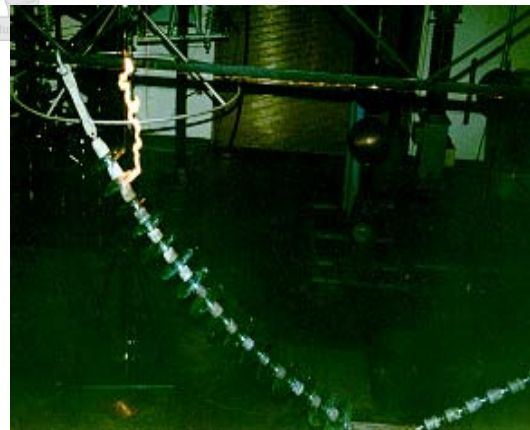


Figure 3.31: Convection of arc

When the clean discs are placed in the middle and at the bottom of the string, similar arcs are observed as in Figure 3.30.

Discussion

The dynamics of the arc produced in these tests were as expected. The arc produced over the “clean” discs has a very high temperature, causing it to rise, and eventually to “creep” towards the top grounded plane. This test was however performed over 3 – 6 seconds, much slower than it would take for the protection of a typical transmission line to trip (30 – 80ms for Zone1 tripping). The thermal effect of the arc during these tests is however very significant, as the observation after an anomalous flashover indicates arcing on the first three to four discs, followed by a flashmark on the tower structure directly above these discs [Britten 1999]. On the other hand, the current levels were much lower than experienced in the field.

3.4.3 Tests done on 275kV tower

Certain tests were attempted on a 275kV tower window, erected outside the High Voltage laboratory, by inserting the V-string insulators into the tower window (see Appendix B).

The tests were practically extremely difficult to achieve, as there was no tension on the insulator string, and consequently it sagged inwards to where the conductor normally hangs. It would thus not be a true reflection of the electric field strength and the voltage profiles within the tower window as experienced during normal operating conditions.

Corona activity was prevalent, but no flashover of the insulator string could be initiated when non-uniformly distributed artificial pollution was applied to the insulator string.

3.5 General summary of laboratory tests

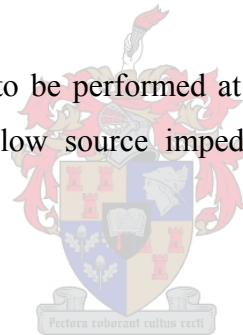
In this chapter various laboratory tests were done to investigate the effect of partial pollution on the performance of glass cap-and-pin insulators.

These tests showed that the fact that the undersides of the glass discs become conductive due to pollution does not contribute to a significant reduction in flashover voltage. It was demonstrated that one or two clean discs in a polluted insulator string may flash over due to voltage transfer by the conducting layer on the polluted discs. The arc however did not develop into a full flashover of the string.

It was also demonstrated that the heat generated by a current carrying conductor may cause the adjacent polluted discs to be drier with a higher resistance than those of the rest of the string.

Several attempts to induce flashover of 275kV strings due to uneven pollution of the string were unsuccessful. A limitation of the laboratory tests was the high source impedance.

A test was therefor planned to be performed at Koeberg Insulator Pollution Test Station (KIPTS) where the low source impedance could be utilised. This is discussed in the next chapter.



The effect of a spark gap in series with a polluted insulator string

This chapter reports on the investigation of the effect of a spark gap in series with a polluted insulator string [Kleinhans 2000].

The laboratory tests in the previous chapter indicated that flashover may occur on one or two clean discs in an otherwise polluted string. In order to simulate these conditions on a 66kV system, a spark gap was inserted in series with a 66kV insulator string at Koeberg Insulator Pollution Test Station (KIPTS).

4.1 Technical layout and setup of experiments at KIPTS

The equipment for the experiment was set up as shown in Figure 4.1. In the setup, strings A and B are two 6-disc glass cap-and-pin insulator strings.

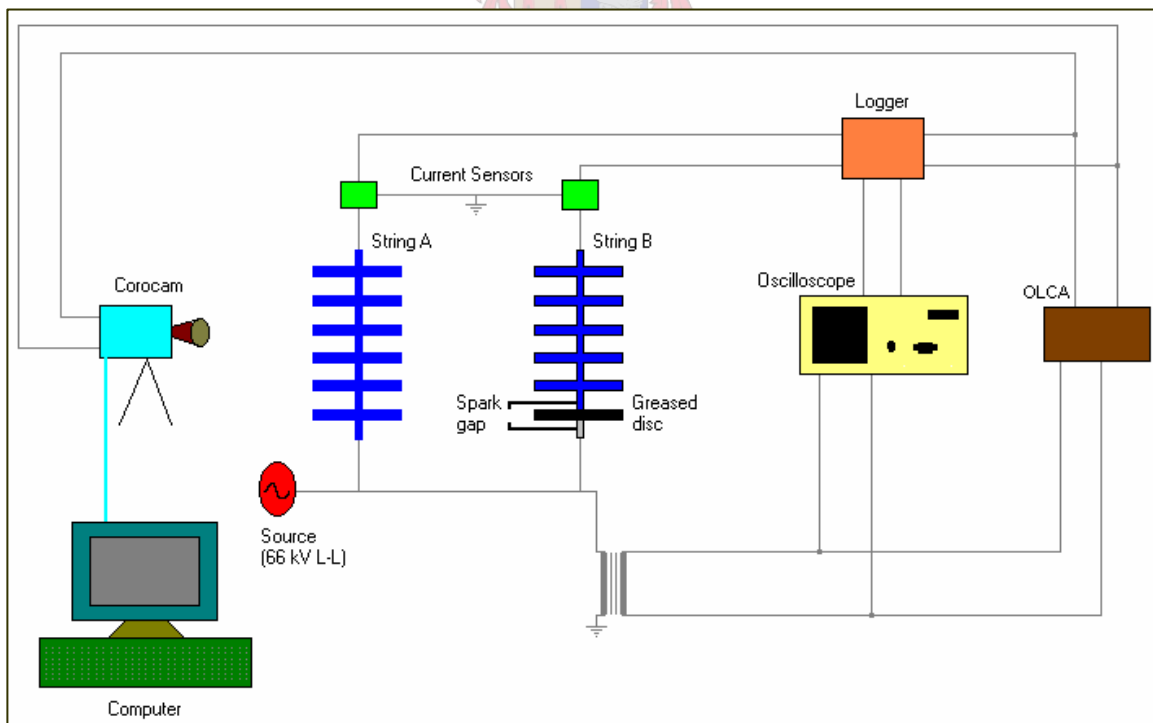


Figure 4.1: Schematic diagram of test setup

These strings were installed at Koeberg Insulator Pollution Test Station (KIPTS) and were allowed to collect pollution naturally under high humidity conditions, as shown in Figure 4.2.

The configuration in string B is implemented by applying silicone grease on the disc at the live end and by fitting a spark gap across this last disc (Figure 4.3). The gap was set to flash over at a voltage of 32 kV, to ensure that it would flash over when 80% of the phase to ground voltage appears across the gap.

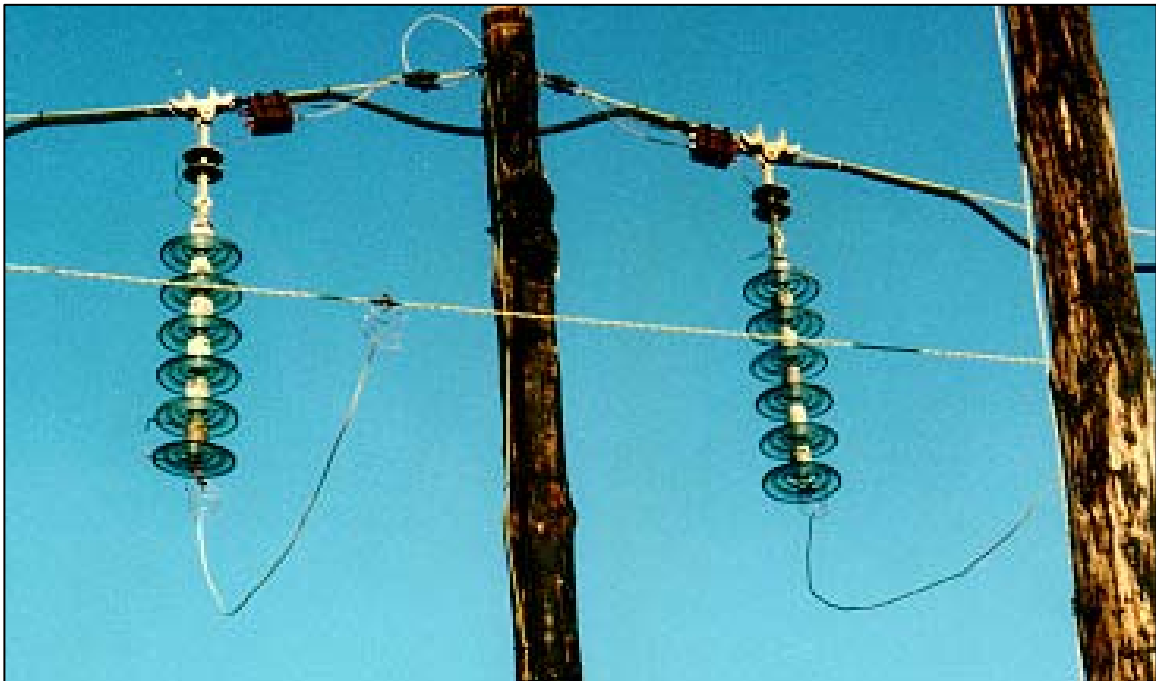


Figure 4.2: Actual setup at KIPTS

Two current sensors are placed on the earthed end of the insulator strings to measure the leakage current flowing over the discs. The sensor consists of a Hall-effect current sensor and other logic to convert the leakage current into a measurement voltage. These measurement voltages are connected via a logger to a 400 MHz oscilloscope, a 2 kHz OLCA (on-line leakage current analyser) and the 10 kHz Corocam in parallel. When partial breakdown of air thus occurs over the spark gap, the Corocam would also be triggered for this event. The operating voltage (66 kV L-

L) was measured via a VT by the above mentioned equipment, to correlate the leakage current with the operating voltage, especially with respect to phase shift.



Figure 4.3: Spark gap used in experiment

Both strings are subjected to normal ambient pollution. The greased disc on string B however blocks the flow of leakage current until the gap across it flashes over. String B is considered an extreme case of non-uniform pollution.

4.2 Results of measurements

The leakage current for both strings are measured and compared. The test was run continuously for 16 days. The relative humidity during the evenings, when all of the measurements were taken, was on average higher than 80%.

String A

On string A, the leakage current observed is depicted in Figures 4.4 and 4.5 respectively.

String B

The leakage current over string B was different to that observed over string A. A very small capacitive current was observed (Figure 4.6) flowing continuously over the insulator surface.

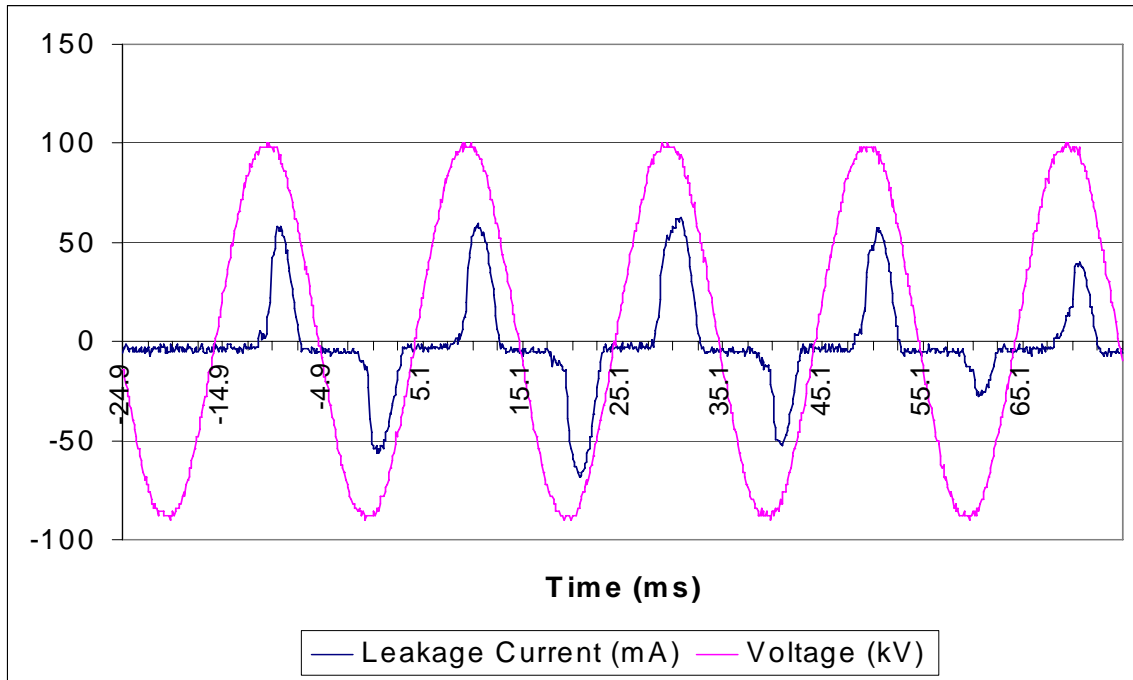


Figure 4.4: Leakage current over string A – oscilloscope

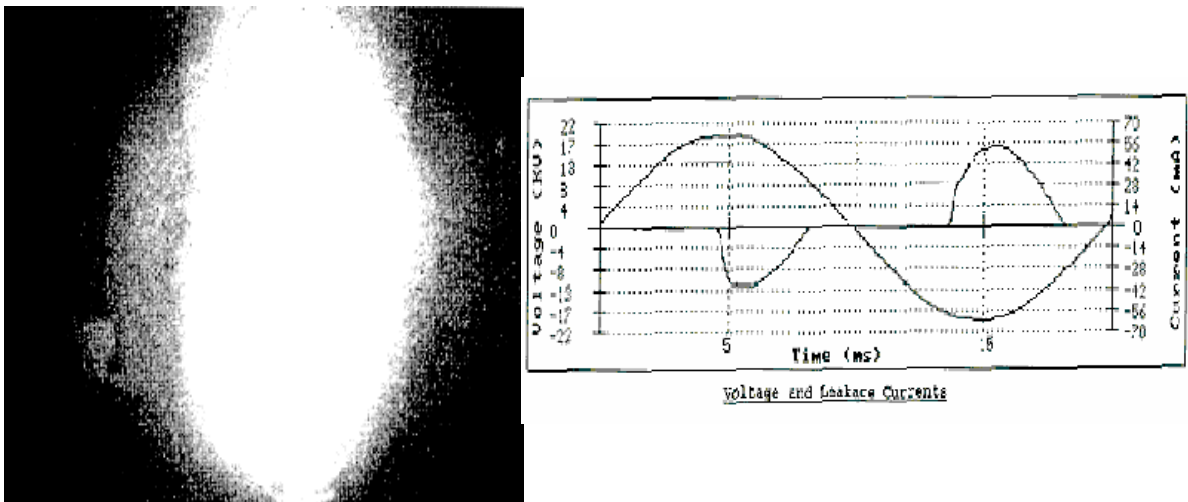


Figure 4.5: Leakage current over string A – Corocam and OLCA

However, on rare occasions, the spark gap would flash over, and the following waveform is observed (Figure 4.7).

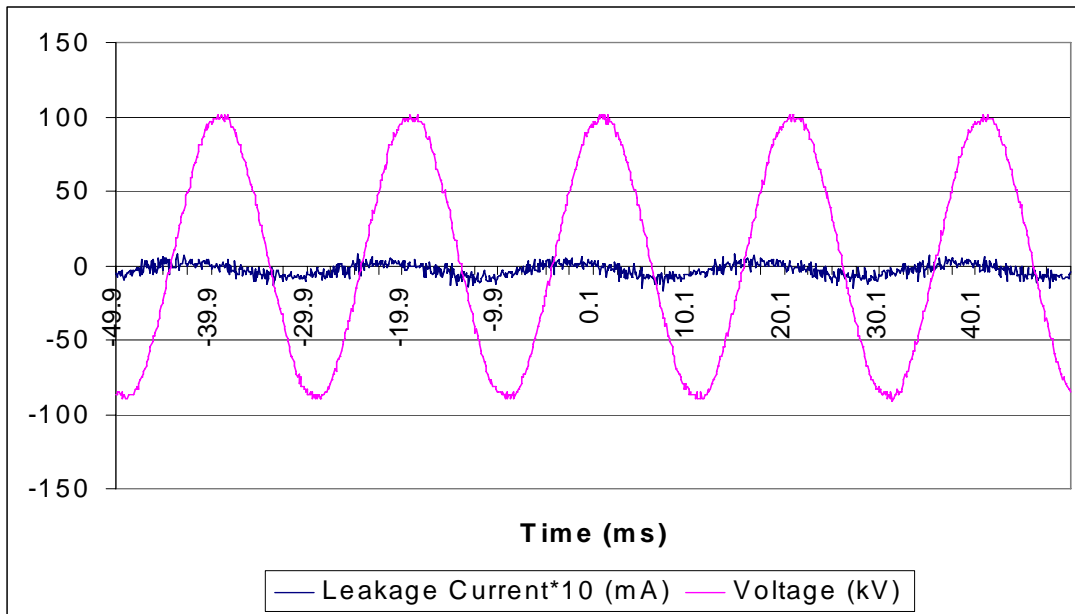


Figure 4.6: Small capacitive leakage current over string B – oscilloscope

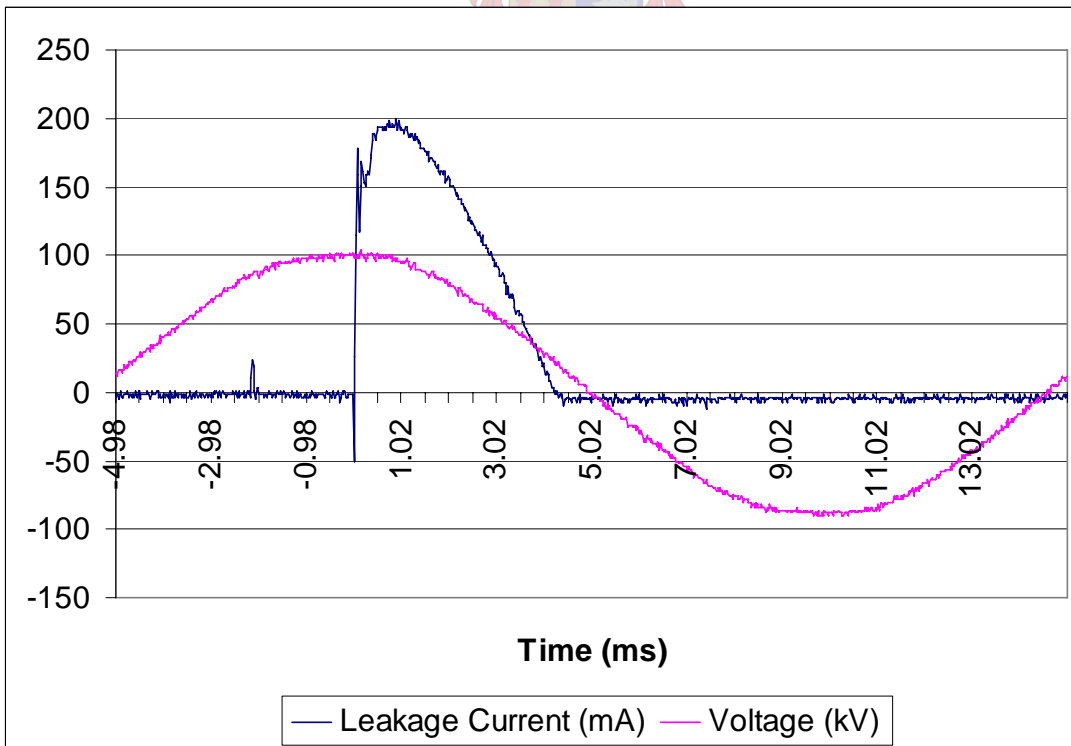


Figure 4.7: Spark gap flashover on string B - oscilloscope

Frequently, small discharges would occur in the pin area of specific discs.

4.3 Discussion

The equivalent circuits of the two strings are depicted in Figure 4.8.

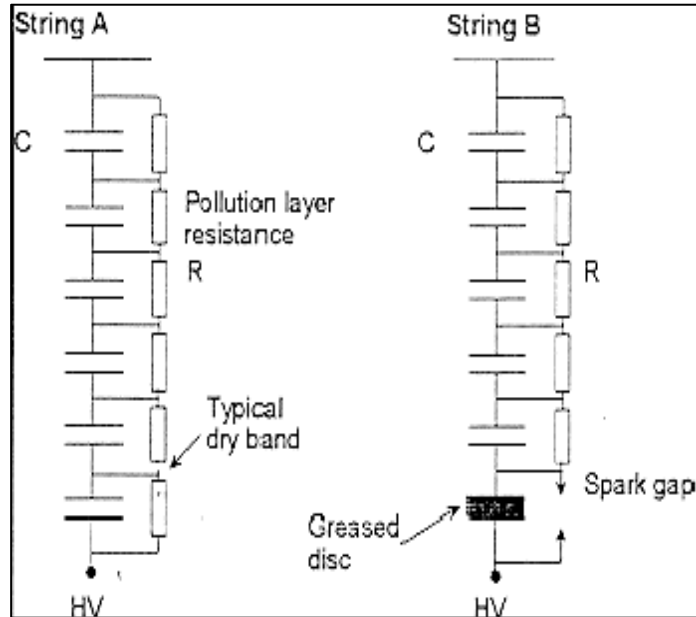


Figure 4.8: Equivalent diagram of the two insulator strings

String A:

The waveform of the leakage current obtained by the oscilloscope and the Corocam clearly indicates that a resistive current is flowing over the insulators. The maximum leakage current observed over this period was 100mA. The resistance of each disc is thus from Figure 4.8:

$$R = \frac{V}{I} = \frac{53.89kV}{100mA} = \frac{539k\Omega}{6(discs)} = 90k\Omega / disc \quad (4.1)$$

The conductivity of the pollution layer on each disc is given by:

$$\sigma_s = \frac{f}{R} = \frac{0.7}{90k\Omega} = 7.8\mu S \quad (4.2)$$

where f is the form factor for a U102BS glass cap and pin insulator.

From these waveforms, it is also observed that a large amount of energy is dissipated (I^2Rt losses), which incites the formation of dry bands. This is typical of the classical pollution flashover phenomenon.

String B:

Initially, the silicone grease blocks the current flowing over the insulator string. On this string a very small capacitive current is observed (in the order of 0.5mA). This is possibly due to the very big reactance of the greased disc.

The impedance of the string is thus from Figure 4.8:

$$Z = \frac{v}{i} = \frac{53.89V}{0.5mA} = 107.8M\Omega \quad (4.3)$$

As observed, the leakage current flowing is almost purely capacitive (Figure 7.6), thus

$$C = \frac{1}{\omega Z} = \frac{1}{2 * \pi * 50 * 107.8M\Omega} = 29.5pF \quad (4.4)$$

This is the same as the capacitance of one clean disc. The leakage current is thus totally dependent on the capacitance of the greased disc, as shown in Figure 4.8.

Small discharges appear at the pin areas of one or two discs without the spark gap flashing over. This is due to the high electric field strength in these regions. These small discharges reached values of up to 25mA, and could visually be observed on the insulator string.

Voltage transfer does however take place over the string. The spark gap flashes over from time to time, and only under certain conditions. When it does flash over, the current waveform initiates at V_{max} , and has a rise time of $\approx 100\mu s$ and a fall time of $\approx 7ms$. The amplitude of the wave is often also 400% bigger than those observed on string A. From the data of Figure 4.7, the resistance of the string at time of flashover (ignoring the resistance of the arc) is:

$$R = \frac{V}{I} = \frac{53.89kV}{250mA} = 216k\Omega \quad (4.5)$$

For one disc:

$$R = \frac{216k\Omega}{5discs} = 43k\Omega \quad (4.6)$$

since the arc shorts out the disc at the live end, as is evident from Figure 4.8. The conductivity of the pollution layer is therefore:

$$\sigma_s = \frac{f}{R} = \frac{0.7}{43k\Omega} = 16\mu S \quad (4.7)$$

From this data it is clear that the conductivity of the discs on string B is almost twice as high as that of string A. The greased disc blocks the flow of leakage current and thus prevents the drying out of the pollution layer – unlike in the case of string A.

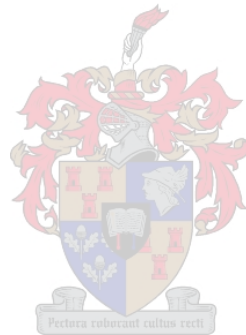
Therefore, when the gap flashes over, the resulting leakage current has a higher magnitude than in the case of string A. Eventually, two weeks after these tests were started, string B flashed over (the Mace fuse blew at 0.7 A).

This experiment was done at 66kV line voltage (38kV L-G). At a much higher voltage such as 275 kV, a similar phenomenon could occur where one or two clean discs of an otherwise polluted string perform the function of the spark gap [Kleinhans Holtzhausen Vosloo, 1999]. The flashover of the clean discs in effect applies the full voltage (minus the arc voltage) to the low resistance length of the rest of the string. This may initiate flashover, to that caused by switching impulses on a polluted string [Ely Roberts, 1968 & Garbagnati Marrone Porrina Perin Pigni, 1987].

4.4 Conclusions

- There is a definite difference in leakage current waveforms between the classical pollution flashover and the spark gap flashover due to voltage transfer over the insulator surface.

- More energy is dissipated during a pollution flashover than with the spark gap flashover, however, the current peaks are much lower and stable in the case of pollution flashover.
- The conductance of the insulator string with the spark gap (string B) is higher than that of string A.
- At higher voltages, the spark gap can be seen as a localised flashover over one or two glass discs, as was observed in the previous chapter. With much higher leakage current peaks expected, more research should be done in order to determine the effect of such occurrences.



Conclusions

The most important conclusions of each chapter are summarised in this chapter. The possible way forward to proving the hypothesis is also suggested.

From the literature survey the following conclusions can be drawn regarding a possible light pollution flashover mechanism of 275kV transmission lines as a cause of the unknown outages experienced on the Eskom network:

- Under normal power frequency voltage conditions, air breakdown of a clean insulator string is for all practical purposes impossible. Flashover of a clean insulator string would therefore only be possible due to switching surges, or lightning.
- The pollution flashover phenomenon has been extensively researched. For this hypothesis, however, a light pollution layer together with light wetting is present on the insulator surface. Under normal operating conditions in practice the creepage distance of the 275kV insulator string is close to the lower limit of light pollution conditions. This light pollution and light wetting phenomenon, however, will not cause a flashover under normal voltage conditions.
- There exists a strong possibility that the anomalous flashover phenomenon is caused by a combination of mechanisms involving the pollution and air breakdown flashover mechanisms. Contributory factors could include the high relative humidity (above 75%) and the marginal creepage distance along the insulator strings.
- The effect of such a combination of factors on the voltage distribution along the insulator string, the electric field in the vicinity of the live end and the flashover voltage is apparent.

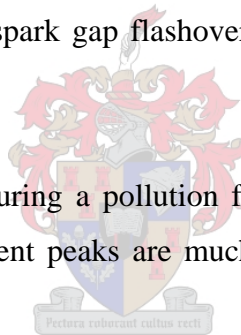
The following conclusions could be drawn regarding the laboratory tests performed:

- When flashover tests are performed on a 4-disc glass insulator string, there exists a linear reduction in value between the flashover voltage and the dry arcing distance (DAD). When these results are extrapolated to a 16-disc glass insulator string, it does not explain the phenomenon of the anomalous flashovers.
- At the fixed voltage of 50kV used for potential and electric field distribution tests along a 4-disc glass insulator string, the tests indicate a reduction in voltage from a clean insulator string if specific glass discs are polluted. The highest potential difference as well as electric field strength is situated across clean discs that are adjacent to polluted discs. Even though the electric field strength is much less than the breakdown strength of air, at higher voltages this could lead to the breakdown of air and resultant localised flashover across this clean disc.
- The voltage and electric field distribution over a clean 16-disc glass insulator string clearly indicates that field enhancement occurs across the two clean discs. This is to be expected as the pollution layer in fact “applies” the full voltage across the two clean discs. These tests also confirm that the value of the conductivity of the pollution layer has little effect on the voltage and electric field distribution. The localised flashover phenomenon could be explained, yet full flashover could not be achieved.
- During the night tests done on the 16-disc glass insulator string the results indicate a large temperature and resistance increase in the region of the “live end” of the insulator string. Using the previous results, it could be postulated that when a voltage is applied to the conductor, taking only temperature into account, the line to ground voltage would be over the “live end” disc causing a localised flashover. At lower temperatures of the conductor (between ambient and $\pm 50^{\circ}\text{C}$) no temperature differences as seen from above tests were observed. Thus at normal operating conditions the above phenomena in itself would not cause an anomalous flashover.

- The tests done on the 25kV V-string traction insulator demonstrated the postulated effects of the hypothesis on a smaller scale, as it was not possible to do so with a 32-disc glass insulator string. These tests did not show any results, but it should be noted that using different methods, i.e. constructing a bigger dry-ice box could have resulted in a different outcome.
- Tests done on the 32-disc V-string showed that the dynamics of the arc produced in these tests were as expected. It however did not develop into a flashover of the insulator string. This could be due to the limited power of the input source to the High Voltage Laboratory.

The results of the tests performed at KIPTS are interpreted as follows:

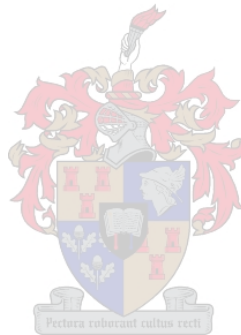
- There is a definite difference in leakage current waveforms between the classical pollution flashover and the spark gap flashover due to voltage transfer over the insulator surface.
- More energy is dissipated during a pollution flashover than with the spark gap flashover, however, the current peaks are much lower and stable in the case of pollution flashover.
- At higher voltages, the spark gap can be seen as a localised flashover over one or two glass discs, as was observed in the previous chapter.



The laboratory and KIPTS tests have not proven the non-uniform light pollution flashover mechanism successfully, however a way forward is suggested:

- According to Holtzhausen and Vosloo, an air breakdown flashover mechanism in light pollution conditions is proposed. This hypothesis explains that, as in the case of section 3.3, the polluted part of the insulator string has a specific non-uniform distribution. Full scale testing in conditions similar to the normal operating conditions is proposed to prove the validity of this hypothesis.

- In section 3.3.2, the temperature and resistance measurements revealed a possible mechanism that could cause the drying of the live end disc. Full scale testing should be done on insulators where this phenomenon is demonstrated together with an applied line voltage. The consequent voltage and electric field measurements should be taken and compared to the results obtained above.
- Electric field simulations should be done using a 3D-software simulation package. The effect on the electric field in the above setups should be studied further to understand the effect on the voltage profile along the insulator string.



BIBLIOGRAPHY

<u>Authors</u>	<u>Publication</u>
Abdel-Salam M., Anis H., El-Morshedy A., Radwan R.	“High-Voltage Engineering, Theory and Practice, Second Edition, Revised and Expanded”, Marcel Dekker, Inc.
Al-Hamoudi I. Y.	“Performance of high voltage insulators under heavy natural pollution conditions”, Power Transmission Department, SCECO-East October 1995.
Allen N. L. , Boutlendj M. , Lightfoot H. A.	Dielectric breakdown in non-uniform field air gaps”, IEEE transactions on electrical insulation, Vol. 28, No. 2, April 1993.
ANSI	“Wet-process porcelain and toughened glass – Suspension type”, ANSI C29.2 – 1992.
Boehne E. W. , Weiner G. S.	“Contamination of EHV insulation – I: An analytical study”, For presentation at Summer Power Meeting, L.A., July 1966.
Bologna F. F.	“Sasolburg insulator pollution test station 1996”, Eskom internal report, TRR/E/96/EL192.
Bologna F. F.	“Insulator leakage currents under light pollution and light wetting conditions: Progress report on initial tests done at NEFTA”, Eskom internal report, TRR/E/98/EL045, March 1998.
Britten A. C.	“Rogue line study: progress report”, Eskom internal report, June 1997.
Britten A. C. , Bekker H. J. J. , Bologna F. F. , Stevens D. J. , Watridge G. M.	“Light pollution on glass disc insulators as an underlying cause of flashovers in Eskom’s 275 and 400kV networks”, ISH’99, Vol. 4, Topic F, Section (d) – Polluted insulators, August 1999.

Burger A. A	“Dielectric tests on insulation for Harvard-Merapi and Georgedale-Venus 275kV lines”, Eskom Transmission Line Technology internal report, 24 July 1997.
Burnham J. T.	“Bird streamer flashovers on FPL transmission lines”, Paper 94 SM 461-4PWRD presented at the IEEE Summer meeting, April 1994.
Cockbaine D. R.	“Remote reading AC fieldmeter”, University of Witwatersrand – Johannesburg, March 1988.
Diab R. D. , Common S. , Roberts L. M.	“Power line insulator pollution and power dips in Natal, South Africa”, Atmospheric Environment, Vol. 25A, No. 10, pp.2329-2334, 1991.
EPRI	“Transmission line reference book: 345kV and above”, Second Edition, EPRI, 1982.
EPRI	“Transmission line reference book – 345kV and above”, Second edition, Revised, EPRI, 1987.
Eskom	Eskom Statistical Yearbook 1996.
Fedan F. M. et al	“Performance of HV transmission line insulators in desert conditions: review of research and methods adopted internationally”, IEEE Trans. On Elec. Ins., Vol. E-18, No. 2, April 1983.
Forrest J. S.	“The electrical characteristics of 132kV line insulators under various weather conditions”, pp. 401-433, 1936.
Forrest J. S. , Lambeth P. J. , Oakeshott D. F.	“Research on the performance of high-voltage insulators in polluted atmospheres”, IEEE paper no.3014 S, November 1959.
Glover J. D. , Sarma M.	“Power system analysis and design”, ISBN 0 53493 950 0.
Guror R. S. , Cherney E. A. , Burnham J. T.	“Outdoor insulators”, USA.
Guror R. S. , De La O A. , El-Kishky H. , Chowdhary M. , Mukherjee H. , Sundaram	“Sudden flashovers of non-ceramic insulators in artificial contamination tests”, IEEE transactions on dielectrics and electrical insulation, Vol. 4, No. 1, February 1997.

R.	
Hampton B. F.	“Flashover mechanism of polluted insulation”, Proc. Inst. Elec. Eng. (London), Vol. 111, pp. 985-990, May 1964.
Harada T. , Aoshima Y. , Ishida Y. , Ichihara Y. , Anjō K. , Nimura N.	“Influence of air density on flashover voltages of air gaps and insulators”, IEEE transactions on power apparatus and systems, Vol. PAS-89, No. 6, July/Aug. 1970.
Hileman, A. R.	“Insulation Coordination for Power Systems”, Marcel Dekker Inc., 1999.
Holtzhausen J. P.	“An introduction into high voltage engineering”, Eskom course: Module 11797, University of Stellenbosch, 1996.
Holtzhausen J. P. , Vosloo W.L.	“The AC Flashover of a 275 kV glass cap and pin Insulator String under light non-uniform Pollution: a Hypothesis”, IASTED International Conference: Power and Energy Systems (PES 2000), Marbella, Spain, September 2000.
IEC report	“Artificial pollution tests on high voltage insulators to be used on AC systems”, CEI IEC 507, Second edition, 1991-04.
IEC report	“Guide for the selection of insulators in respect of polluted conditions”, Publication 815, First Edition, 1988.
IEEE Standard 4-1978	IEEE Standard Techniques for High-Voltage Testing, pp. 27-29, IEEE Power Engineering Society.
Johnson J. , Henderson R. T. , Price W. S. , Hedman D. E. ; Turner F. J.	“Field and laboratory tests on contaminated insulators for the design of the State Electricity Commission of Victoria’s 500kV system”, IEEE transactions on power apparatus and systems, Vol. PAS-87, pp. 1216-1239, May 1968.
Kawai M.	“Tests in Japan on the performance of salt-contaminated insulators in natural and artificial humid

	conditions”, IEEE proceedings, Vol. 115, No. 1, January 1968.
Kawai M. , Milone D. M.	“Tests on salt-contaminated insulators in artificial and natural wet conditions”, IEEE transactions on power apparatus and systems, Vol. PAS-88, No. 9, September 1969.
Kawamura T. , Isaka K.	“Humidity dependence of moisture absorpsion, leakage current and flashover voltage on comtaminated surfaces”, Electrical engineering in Japan, Vol. 93, No. 5, 1973.
Khalifa M.	“High-voltage engineering: Theory and practice”, ISBN: 0 8247 8128 7, USA.
Kind D. , Kärner H.	“High-Voltage Insulation Technology, Textbook for Electrical Engineers”, Friedr. Vieweg & Sohn.
Kleinhans K. D., Holtzhausen J. P., Vosloo W. L., Britten A. C.	“The effect of a spark gap in series with a polluted insulator string”, SAUPEC 2000, Durban, 2000.
Kleinhans K. D., Holtzhausen J. P., Vosloo W. L.	“The effect of inserting two clean discs in a polluted 275 kV AC string: An experimental investigation”, ISH’99, London, 1999.
Leob L.	Electrical Coronas – Their Basic Physical Mechanisms, Berkeley, CA: University of California Press, 1965.
Looms J. S. T.	“Insulators for high voltages”, IEE Power Engineering Series 7, ISBN 0 86341 116 9, 1988.
Maecker H. H.	“Principles of arc motion and displacement”, Proceedings of the IEEE, Vol. 59, No. 4, April 1971.
Malik N. H. , Al-Arainy A. , Qureshi M. I.	“Electrical insulation in power systems”, Power engineering series, ISBN: 0 8247 0106 2.
McElroy A. J. , Lyon W. J. , Phelps J. D. M. , Woodson H. H.	“Insulators with contaminated surfaces; Part I: Field conditions and their laboratory simulation”, IEEE transactions on power apparatus and systems, Vol. PAS-89, No. 8, Nov./Dec. 1970.
Näche H.	“Stabilitat der fremdschichtentladunger und theorie des

	fremdschichtrüberschlags”, Elektrotech. Z. Augs. A, Vol. 16, pp. 577-585, August 1966.
Naito K. , Matsuoka R. , Ito S. , Morikawa S.	“An investigation of the horizontally mounted insulators for HVDC stations”, IEEE transactions on power delivery, Vol. 4, No. 1, January 1989.
Pei-zhong H. , Cheng-dong X.	“The test and investigation results on naturally polluted insulators and their application to insulation design of power system in polluted areas”, CIGRE 33-07.
Pilkington Glass Catalogue for U70&U120	Power-frequency and impulse voltage withstand and flashover of number of insulators per string.
Reece T. A. , Mauldin T. P. , Hillesland T. , Knudsen S. R.	“PG&E’s cool fog tests on artificially contaminated suspension insulators”, IEEE PES Winter Meeting, paper T 74 070-9, 1974.
Reynders J. P.	“Guide to the choice of outdoor insulators for AC systems under polluted conditions”, NEC division: Electrical energy, Pr. no. ELEK3, 1992.
Riquel G. , Spangenberg E. , Mirabel P. , Saison J. Y.	“Wetting processes of pollution layer on high voltage glass insulators”, 9 th ISH, Graz – Austria, pp3190-1-4, August 1995.
Rizk F. A. M.	“Mathematical models for pollution flashover”, Electra-technical papers, No. 78, pp. 71-103.
Rizk F. A. M. , Beausejour Y. , Shi Xioung H.	“Sparkover characteristics of long fog-contaminated air gaps”, IEEE transactions on power apparatus and systems, Vol. PAS-100, No. 11, November 1981.
Rizk F. A. M. , El-Sarky A. A. , Assaad A. A. , Awad M. M.	“Comparative tests on contaminated insulators with reference to desert conditions”, CIRGE 1972 Session, Paper no. 33-03, 1970.
Rizk F. A. M. , Kamel S. I.	“Modelling of HVDC wall bushing flashover in non-uniform rain”, IEEE transactions on power delivery, Vol. 6, No. 4, October 1991.
Rogue line working group – Eskom	“Rogue line working group: brief notes of meeting”, TRI – Rosherville, 11 February 1999.
Ryan H. M.	“High voltage engineering and testing”, IEE Power

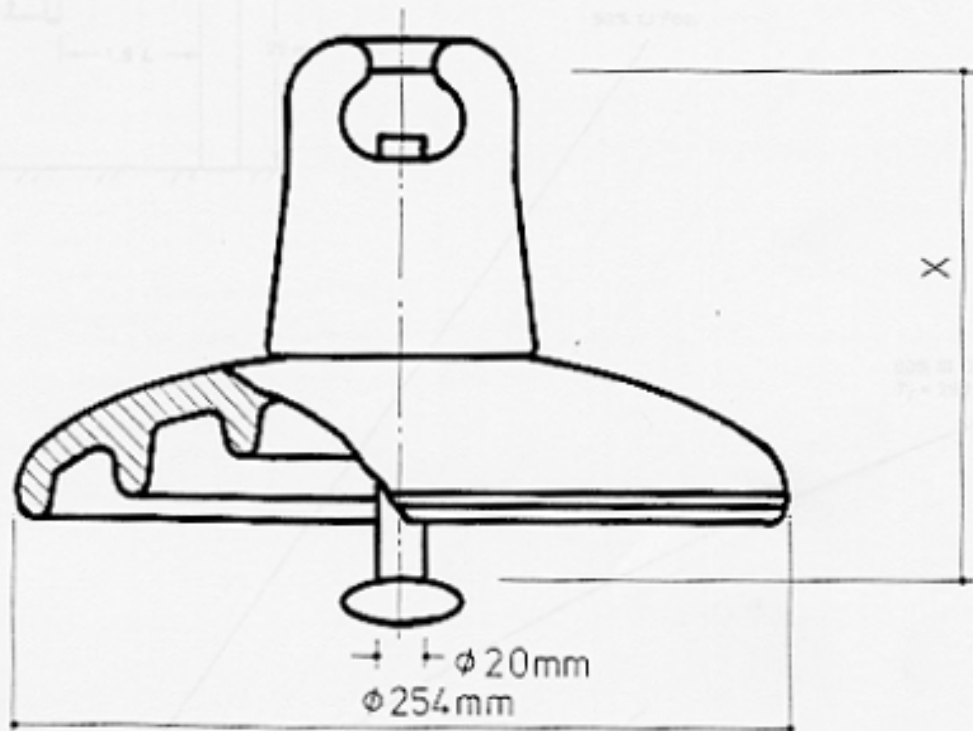
	Series 17, Peter Peregrinus Ltd.
Schnieder H. M. , Lux A. E.	“Mechanism of HVDC wall bushing flashover in non-uniform rain”, IEEE transactions on power delivery, Vol. 6, No. 1, January 1991.
Standring W. G.	“Some measurements on the electrical characteristics of insulator strings”, Transactions of the American IEE, November 1932.
Swift D. A.	“Pollution flashover performance of ceramic high-voltage insulators: A critique of using solely specific leakage distance for dimensioning purposes”, SAUPEC paper, 1996.
Swift D. A.	“Flashover across the surface of an electrolyte: Arresting arc propagation with narrow metal strips”, IEE proceedings, Vol. 127, Pt. A, No. 8, November 1980.
Tang L. , Raghuveer M. R.	“Modelling of HVDC wall bushing flashover due to uneven wetting”, IEEE transactions on power delivery, Vol. 14, No. 1, January 1999.
Taylor P.	“Kwazulu-Natal birg guard project review”, Eskom internal report, January 1999.
Taylor P. , Naidoo P. , Hoch D.	“Investigation into transient earth faults on the Geordedale-Venus 275kV transmission lines”, Eskom internal report, July 1996.
Van Olphen H.	“Clay colloid chemistry”, New York: Interscience, 1963.
Vlastós A. E.	“Breakdown of air in the non-homogeneous field”, Proceedings of IEE, Vol. 113, No. 5, May 1966.
Vosloo W. L.	“Introduction to insulator pollution monitoring in distribution and transmission power networks”, Eskom – Distribution: Technical training report DCTT/TM 044, rev. 0, November 1996.
Vosloo W. L. Bologna F. F.	“High voltage insulators: the backbone of transmission and distribution networks.”

Weeks W. L.	“Transmission and distribution of electrical energy”
West H. J. , Brown J. E. , Kinyon A. L.	“Simulation of EHV transmission line flashovers initiated by bird excretion”, Paper 71 TP 145-PWR presented at the IEEE PES Winter meeting, February 1971.
West H. J. , McMillan D. W.	“Fire induced flashovers of EHV transmission lines”, Paper A 79 047-2 presented at IEEE PES Winter meeting, February 1979.
Woodson H. H. , McElroy A. J.	“Insulator with contaminated surfaces; Part II: Modelling of discharge mechanisms”, IEEE transactions on power apparatus and systems, Vol. PAS-89, No. 8, Nov./Dec. 1970.
Yamakazi K. , Mita N. , Tomiyama J. , Miyoshi Y.	“Counter measures against salt pollution insulators used for EHV transmission systems”, CIGRE, Paris, paper 412, 1958.
Yamamoto M. , Ohashi K.	“Salt contamination of external insulation of HV apparatus and its countermeasures”, Trans. Amer. Inst. Elec. Engrs., vol. 80, p.380, 1961.
Zoledziowski Z.	“Time-to-flashover characteristics of polluted insulation”, IEEE transactions on power apparatus and systems, Vol. PAS-87, No. 6, June 1968.

Appendix A: Type of glass insulator used in tests



U120BS/20



INSULATOR TYPE
INSULATING MATERIAL
COUPLING METHOD
LOCKING DEVICE

U120BS/20
TOUGHENED GLASS/GETEMPERDE GLAS
20 mm BALL & SOCKET/KOELWRIJ
20 mm "W" TYPE SECURITY CLIP/
"W"-TIPS VEILIGHEIDSKLEM

ISOLATOR TYP
ISOLASIE MATERIAAL
KOPPELINGSMETODE
VEILIGHEIDSKLEM

SHELL DIAMETER
CONNECTING LENGTH "X"
CREEPAGE DISTANCE
PROTECTED CREEPAGE DISTANCE
DRY ARCING DISTANCE
POWER-FREQUENCY DRY F.O. VOLTAGE
POWER-FREQUENCY WET F.O. VOLTAGE
POWER-FREQUENCY ONE MINUTE DRY WITHSTAND VOLTAGE
POWER-FREQUENCY ONE MINUTE WET WITHSTAND VOLTAGE

254 mm
146 mm
180 mm
175 mm
190 mm
70 kV
50 kV
65 kV
43 kV
100 kV
100 kV
100 kV
100 kV
UNPUNCTURABLE/DEURSLAGBESTAND
1,5 x Corr. F.O.
100 kN
28 kN
50 kN
4,7 kg

SKYDIAMETER
KOPPELLENTE "X"
KRUIPAFSTAND
BESKERMDEKRUIPAFSTAND
DROEGOORSLAGAFSTAND
DROEKRAGFREKWENSIE-OORSLAGSPANNING
NATKRAGFREKWENSIE-OORSLAGSPANNING
EEN-MINUUT-DROEKRAGFREKWENSIE BESTANDHEIDSPANNING
EEN-MINUUT-NATKRAGFREKWENSIE-BESTANDHEIDSPANNING

50% LIGHTNING IMPULSE FLASHOVER - POSITIVE
50% LIGHTNING IMPULSE FLASHOVER - NEGATIVE
LIGHTNING IMPULSE WITHSTAND VOLTAGE - POSITIVE
LIGHTNING IMPULSE WITHSTAND VOLTAGE - NEGATIVE
IMPULSE OVERVOLTAGE IN AIR
POWER-FREQUENCY PUNCTURE WITHSTAND IN OIL
MINIMUM MECHANICAL STRENGTH
RECOMMENDED MAXIMUM WORKING LOAD
ROUTINE PROOF TESTING LOAD
MASS PER UNIT

50% BLITSIMPULSOORSLAGSPANNING - POSITIEF
50% BLITSIMPULSOORSLAGSPANNING - NEGATIEF
BLITSIMPULSBESTANDHEIDSPANNING - POSITIEF
BLITSIMPULSBESTANDHEIDSPANNING - NEGATIEF
IMPULSOORSPANNING IN LUG
KRAGFREKWENSIEDEKURSLAGBESTANDHEID IN OLIE
MINIMUM MEGANIESE STERKTE
AANBEVOLE MAKSIMUM BEDRIEFSLAS
ROETINE PROEFSLAS
MASSA-EENHEID

Values are determined in accordance with SABS 177, at an altitude of 1460 metres above sea level and are given as Corrected to Standard Atmospheric conditions (2V 809). All the insulators are manufactured under and carry the S.A. Bureau of Standards Standardisation "Mark", and comply in all respects to SABS 177, BS 137 and IEC 383.

Waardes is volgens SABS 177 by 'n hoogte van 1460 m bo seevlak bepaal en word as gekorrigeer tot standaard atmosferiese omstandighede (kV 809) gegee. Alle insulatore word vervaardig onder en dra die S.A. Buro vir Standaarde se Standaardisatie "Merk" en voldoen in alle opsigte aan SABS 177, BS 137 en IEC 383.



Figure B.1: 275kV tower window set up outside the High Voltage Laboratory

Pollution test methods [EPRI “Transmission Line Reference Book”] may be roughly classified into three categories: salt-fog test, wet-contaminant test and clean-fog test. Each test method essentially simulates a different phenomenon.

The salt-fog test, wet-contaminant test and some clean-fog tests have been established on the assumption that the surface of the contaminated insulator is already wet and conductive when voltage is applied. A different approach is taken for some other clean fog tests, in which a wetting condition, usually fog, is applied to the energised dry insulators. Different assumptions are also made regarding the manner in which the contaminant is deposited on the surfaces of insulators. For instance, the salt-fog method represents a condition in which the contaminant is deposited on the insulators together with moisture, whereas other test methods represent a condition in which the contaminant and moisture are deposited on the insulators at two different times.

The Salt-fog method [IEC report 60507]

In this method, the insulator is energised at service voltage, which is held constant through the test, and subjected to a salt-fog. The salt-fog salinity defines the severity of the contamination. The fog is produced by arrays of nozzles on all sides of the insulator to be tested, directing a fog of droplets at the insulator by means of compressed air. The highest salinity at which there is a withstand in at least three out of four one-hour tests is called the withstand salinity and is regarded as the criterion of performance.

The Wet-contaminant method

In this method, the insulators are contaminated by spraying or flow-coating the contaminant mixture onto the insulator surface. Voltage is applied three to five minutes after the end of the contamination procedure, while the insulators are still wet. In one type of test, the test voltage is increased until flashover occurs. In another type of test, the test voltage is increased at a constant rate to an anticipated value and held at that value until flashover occurs or until the insulator surface becomes dry, and scintillation activity disappears.

Two different types of contaminant slurry are in use today. One has the proportions of 40g of kaolin per liter of water and various amounts of salt (NaCl) to create the desired salt deposit density on the insulator surfaces. The other mixture contains

materials with high viscosity and creates a thicker conducting layer that can remain in a stable, wet condition for a long period of time.

In all tests done during this research study, the former mixture was implemented to obtain the test results.

With both types of slurry, a relatively high flashover strength is found. The wet-contaminant method has an advantage over other methods because of its simplicity, ease of use, and low test cost.

The Clean-fog test method

This method may be separated into two types. The first type, also known as the pre-deposit method [IEEE Standard 4-1978], insulators are contaminated, dried, and then wetted by clean fog. Test voltage is applied to the insulators when leakage resistance has reached its lowest value. Although the procedure is usually classified as a clean-fog test, it should be considered as a variation of the wet-contamination test.

In the second type, voltage is applied to dry contaminated insulators, and then a wetting condition is applied. This procedure is more commonly regarded as a reasonable simulation for natural conditions; however, it is more complicated than the other methods [Kawai 1968 and Kawai Milone 1969]. The wetting condition is usually achieved using steam generated by evaporation of water from open containers. The process of wetting the insulator surface is a key factor in this kind of test. In the slow wetting condition of the steam-fog tests, the surface impedance gradually changes according to the net rate of wetting, which are a function of the humidity in the air and the drying effect of leakage current. This phenomenon would not appear if the rate of wetting were fast enough to overwhelm the drying effect of leakage current.

Comparison of test methods

It is important to understand how contamination test methods differ from each other. Each test method essentially simulates a different phenomenon. A factor that is important for one method may not be significant for other methods. For example, the wetting condition is the most important factor in the clean-fog tests, but not in the wet-contamination tests.

There is no direct relationship between salt-fog, clean-fog and wet-contamination methods, and one single method cannot simulate the breakdown phenomena created

Appendix C: Pollution test methods

by the others. For practical designs, it is extremely important to choose the test method that would simulate the particular natural condition found in service. This was, however, quite difficult seeing that an unknown flashover method is being studied, and only the symptoms of the flashover are known. In most cases, tests were performed during this research using an array of the above test methods, in order to simulate the symptoms shown by the unknown flashovers experienced in the Eskom Transmission network.

An outline of each method is shown in Table C.1.


<i>Test method</i>	<i>Contamination condition</i>	<i>Time or flashover or test duration</i>	<i>Surface condition during test</i>	<i>Remarks</i>
Salt-fog	Contamination and wetting are applied simultaneously by spraying salt water. Degree of contamination defined by amount of salt in solution.	Testing time is 1 hour.	Nearly pure resistive impedance due to the conducting layer on the surface.	Flashover strength linear with string length.
				
Wet-contamination				
1. Light mixture	Defined by amount of dry contaminants.	Flashover after 20-30 seconds.	Wet changing to dry, resistive, and also capacitive impedance in the half-dry condition.	Small regular discs perform better than large discs.
2. Heavy mixture	Defined by surface conductivity.	Flashover within 4-5 seconds.	Wet also at instant of flashover, resistance close to the initial value.	Flashover strength nearly proportional to leakage distance.
Clean-fog				
1. Quick wetting	Defined by amount of dry contaminant.	Test time is 30-60 minutes. Flashover usually within 30 minutes	Dry changing to wet, nearly resistive impedance due to the fast wetting process.	Linear; leakage distance is the main factor.
2. Slow wetting	Defined by amount of dry contaminant.	Test time is 2 hours. Flashover usually after 1 hour.	Dry changing to wet, capacitive and resistive impedance designated as dynamic impedance.	Some non-linearity; large discs are better than small disks.

Table C.1: Comparison of pollution test methods